# INVESTIGATION OF MATHEMATICAL MODELING FOR THE GENERAL TREATMENT OF GLIOBLASTOMA

by

Dharma Raj Khatiwada

A Thesis Submitted to the Faculty of

The Charles E. Schmidt College of Science

in Partial Fulfillment of the Requirements for the Degree of

Master of Science

Florida Atlantic University

Boca Raton, FL

August 2016

**INVESTIGATION OF MATHEMATICAL MODELING FOR THE GENERAL TREATMENT OF GLIOBLASTOMA**

by

Dharma Raj Khatiwada

This thesis was prepared under the direction of the candidate's thesis advisor, Dr. Georgios Kalantzis, Department of Physics, and has been approved by the members of his supervisory committee. It was submitted to the faculty of the Charles E. Schmidt College of Science and was accepted in partial fulfillment of the requirements for the degree of Master of Science.

SUPERVISORY COMMITTEE:

Georgios Kalantzis, Ph.D.
Thesis Advisor

Zoubir Ouhib, M.S., D.A.B.R.

Luc T. Wille, Ph.D.
Interim Chair, Department of Physics

Silvia Pella, Ph.D., D.A.B.R.

Janet Blanks, Ph.D.
Interim Dean, The Charles E. Schmidt College of Science

Deborah L. Floyd, Ed.D.
Dean, Graduate College

07/25/2016
Date

## ACKNOWLEDGMENTS

I would like to thank my Advisor, Dr. Gergeois Kalantzis, Assistant Professor in the Physics Department at FAU who provided the research subject, encouragement and guidance to complete my Thesis.

I am particularly grateful to Dr. Theodora Leventouri, Professor of Physics and Director of the Professional Masters in Medical Physics program for her encouragement, direction and tireless assistance till the final stages of writing the Thesis.

I am thankful to Dr. Silvia Pella, Thesis Committee member, DABR, Wellington Regional Hospital, and Research Affiliate Associate Professor in the Physics Department at FAU for her continued support and guidance in every step of my medical physics studies.

I would like to thank Zoubir Ouhib, Thesis Committee member, MS, DABR of the Lynn Cancer Institute, Boca Raton Regional Hospital, and Research Affiliate Associate Professor in the Physics Department at FAU for his remarkable contribution toward my progress in medical physics studies.

## ABSTRACT


| | |
|---|---|
| Author: | Dharma Raj Khatiwada |
| Title: | Investigation of Mathematical Modeling for the general treatment of Glioblastoma |
| Institution: | Florida Atlantic University |
| Thesis Advisor: | Dr. Georgios Kalantzis |
| Degree: | Master of Science |
| Year: | 2016 |

The purpose of this research is to validate various forms of mathematical modeling of glioblastoma multiforme (GBM) expressed as differential equations, numerically. The first work was involved in the numerical solution of the reaction-convection model, efficacy of which is expressed in terms of survival time. It was calculated using simple numerical scheme for the standard-of-care treatment in clinics which includes surgery followed by the radiation and chemotherapy. Survival time using all treatment options increased significantly to 57 weeks compared to that of surgery close to 14 weeks. It was also observed that survival time increased significantly to 90 weeks if tumor is totally resected. In reaction-diffusion model using simple numerical scheme, tumor cell density patterns due to variation in patient specific tumor parameters such as net proliferation rate and diffusion coefficient were computed. Significant differences were observed in the patterns while using dominant diffusion and proliferation rate separately. Numerical solution of the tumor growth model under the anti-angiogenic therapy revealed some impacts in optimum tumor growth control however it was not significant.

*This thesis is dedicated to my mother and wife.Their support, encouragement, and constant love have sustained me throughout my life.*

**INVESTIGATION OF MATHEMATICAL MODELING FOR THE GENERAL TREATMENT OF GLIOBLASTOMA**

## LIST OF TABLES

## LIST OF FIGURES

# CHAPTER 1

# BACKGROUND

## 1.1 GLIOBLASTOMA MULTIFORME

Gliomas are the most common primary brain tumors which originate from glial cells in the brain. Glioblastoma multiforme (GBM) is the most aggressive form of the glioma (grade IV glioma, WHO). Diagnosis of glioma is very difficult as tumor cells can be found several centimeters away from the bulk tumor that is visible using current imaging techniques like magnetic resonance imaging (MRI) and computed tomography (CT). Even with the current standard of care which consists of surgical resection, radiation therapy concurrent with chemotherapy, followed by maintenance chemotherapy, glioma remains incurable so far. This is mainly due to their resistive nature against therapies and heterogeneous infiltrative nature of tumor cells. Median survival for a patient diagnosed with GBM is 12-15 months [11].

Exact causes of gliomas including its aggressive form, GBM still remain questionable so far.

Some of the possible factors suggested are:

i. Radiation exposure ( accidental exposure with radiation contained in environment itself or from the treatment of primary tumor treated with radiation, before)

ii. Increased use of cell phone ( due to electromagnetic field generated by it)

iii. Head trauma [27]

iv. Exposure with certain chemicals like petrochemicals, pesticides, and formaldehyde

v. Some viruses [28]

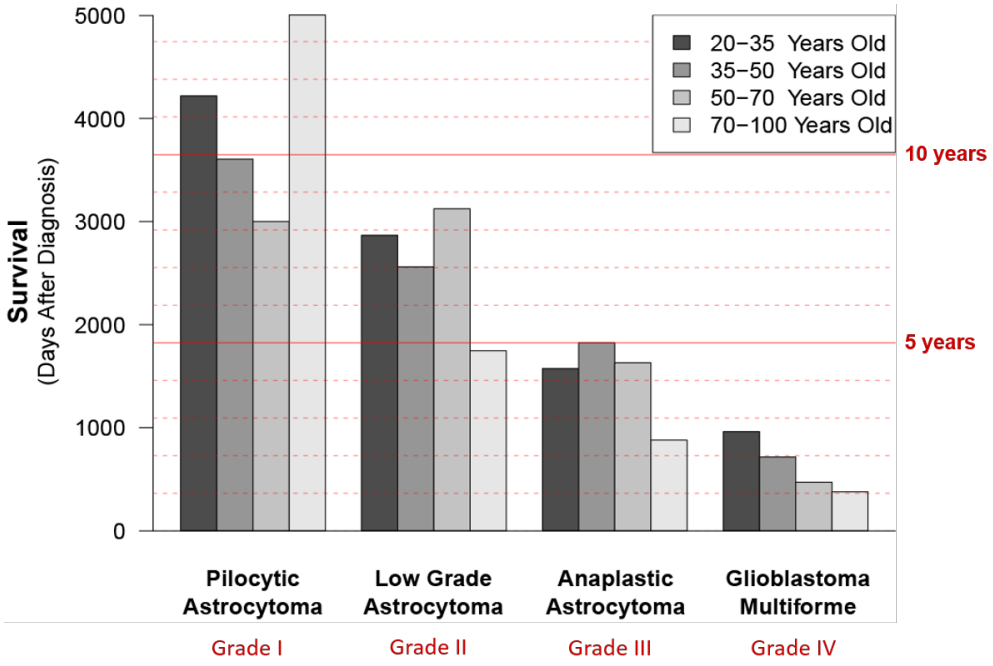


**Figure 1.1**: Survival of patients with the various types of glioma [3]

Figure 1.1 compares survival time of patients at their different age interval with the different types of glioma. Grade levels from I to IV are given by World Health Organization (WHO) based on the nature of gliomas whether they are actively proliferating or stable (benign). Grade I glioma is slowly growing and relatively benign. However growth rate increases with the increase in grade of gliomas. Survival time for grade IV gliomas, glioblastoma multiforme (GBM) is almost 500 days ($\approx$ 10 months) in average for all age classes.

There are three types of normal glial cells that can produce tumors. An astrocyte produces astrocytomas (including glioblastomas), an oligodendrocyte produces oligodendrogliomas, and ependymomas comes from ependymal cells. Tumors that display a mixture of these different cells are called mixed gliomas [1]. The location of the tumor depends on the cells from which it originates.

Figure 1.2 shows various glial cells surrounding a neuronal cell. These non-neuronal cells maintain homeostasis, form myelin, and provide support and protection for the

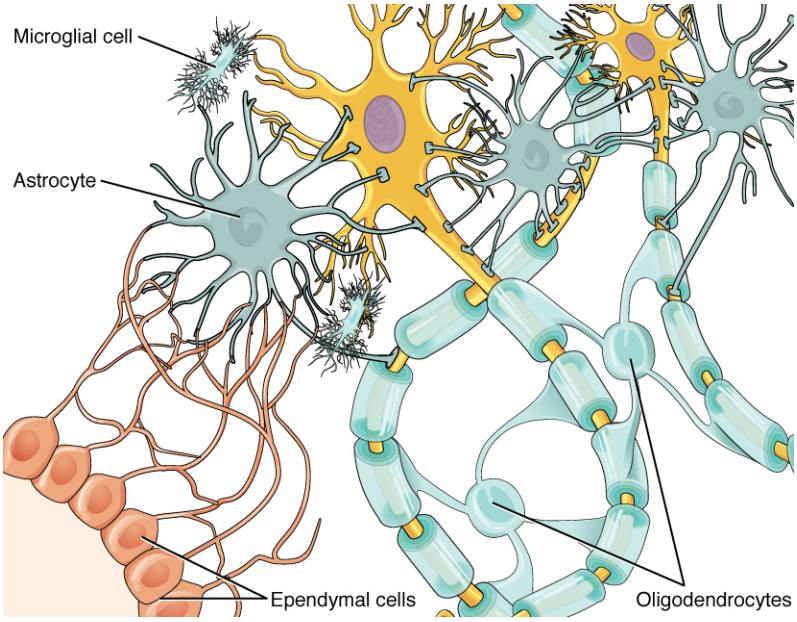


**Figure 1.2**: Envelope of glial cells surrounding neurons in central nervous system [4]

neurons in nervous system.

Various attempts to introduce mathematical models to account for the tumor development have been focused by the following fundamental aspects of tumor:

1. Uncontrolled proliferation of cells
2. Capacity to invade and metastasize [2].

There are various mathematical models in which density of cells or tumor cells density and the concentration of biochemical species (nutrients) are described in terms of differential equations. Some of these models use simple ordinary differential equations, ignoring spatial effects of tumor growth. The model which includes spatial effect also is expressed in terms of partial differential equations (linear/non-linear). Fundamental controlling factors describing these mathematical model based on [2] are net proliferation rate (proliferation rate- death rate) and diffusion coefficient by which tumor cells invade (metastasis) a region otherwise, the region is normally occupied by normal cells. The term diffusion coefficient that accounts for only passive diffusion

(adapted in the most of the simplified mathematical model), is due to gradient-driven Fickian diffusion. In this work, active diffusion due to phenomena like chemotaxis (movement of cells in response to a chemical stimulus) is not considered for mathematical modeling.

Tumor proliferation is due to uncontrolled mitotic growth of cells. The cell cycle shown in Figure 1.3 is the series of events that take place in a cell leading to its division and duplication of its DNA (DNA replication) to produce two daughter cells. It involves a complex series of molecular and biochemical signaling pathways [5].

The cell cycle has four phases:

1. The $G_1$, or gap, phase, in which the cell grows and prepares to synthesize DNA
2. The S, or synthesis, phase, in which the cell synthesizes DNA
3. The $G_2$, or second gap, phase, in which the cell prepares to divide and
4. The M, or mitosis, phase, in which cell division occurs.

There is also a phase outside $G_1$ phase (can also be viewed as an extended $G_1$ phase) called $G_0$ phase in which cells remain quiescent (inactive or dormant). Usually, those cells which lack enough nutrients and proper cellular environment for further division are filtered by checkpoint genes at $G_1$ phase. There are two checkpoints (switches) at $G_1$/S and at $G_2$/M where cells are screened for abnormality if there are any. Those unqualified cells due to damaged DNA or any other defects will be forced to commit suicide which is called apoptosis or programmed cell death. At checkpoints, cells are checked by specialized genes. Due to the defect of regulatory genes in checkpoints, their switching action becomes ON permanently causing uncontrolled growth of cells and leading carcinogenesis or tumor development [5].

Nature of cell proliferation and migration is based on 'Go or Grow Hypothesis' [6]. According to this hypothesis, proliferation and diffusion events are mutually exclusive. At the beginning, tumor starts only proliferating and it goes up to some threshold.

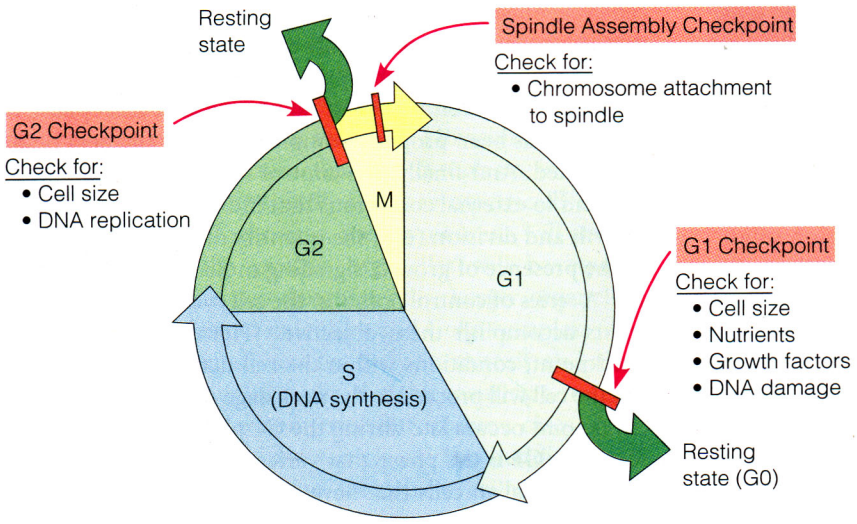


**Figure 1.3**: Schematic diagram of a cell cycle [7]

There is a limitation of vital nutrients that are required for the growth after some time. As a result, some inner cells inside tumor are forced to die (necrosis) and net proliferation rate gets retarded unless angiogenesis (artificially created vascularization) comes into play. Phases of tumor development before and after angiogenesis are termed as avascular and vascular respectively. There is a maximum size of tumor bed called carrying capacity that can be reached with the available nutrients. In another word, this can accommodate all tumor cells resulted from the proliferation during avascular phase. In vascular phase, the carrying capacity also varies with time due to deformation of endothelial cells architecture which forms tumor bed.

# CHAPTER 2

# FORMULATION OF MATHEMATICAL MODELS

## 2.1 ONE DIMENSIONAL MODELS

There are three basic models which account only for the growth (mitotic) of tumor cells volume, the exponential, the logistic, and Gompertz. Contrary to the exponential model, the logistic and the Gompertz models take into account the possible limitation of growth for instance due to, to lack of space or nutrients, assuming that the growth rate depends on the carrying capacity of the environment [8].

The following equations describe above models:

$$\frac{dV}{dt} = \lambda V \qquad \text{(Exponential growth)} \qquad (2.1)$$

$$\frac{dV}{dt} = \lambda V \left(1 - \frac{V}{K}\right) \qquad \text{(Logistic growth)} \qquad (2.2)$$

$$\frac{dV}{dt} = \lambda V \log\left(\frac{V}{K}\right) \qquad \text{(Gompertz growth)} \qquad (2.3)$$

where, V ($mm^3$), $\lambda$ ($day^{-1}$) and K ($mm^3$) are volume, net proliferation rate, and carrying capacity of the basal membrane (which forms tumor bed) respectively. When tumor development enters in vascular phase, there is an increase in cell mass and physical pressure causing deformation and expansion of base membrane (formed by endothelial cells) and ultimately increasing the spatial carrying capacity.

Universally agreed fact, so far regarding angiogenesis, is that after threshold is reached in terms of size, tumor cells secrete angiogenic stimulator like vascular endothelial growth factor (VEGF) which breaks down nearby vascular network (sprouting). Ultimately, nutrient deprived tumor cells feed on such neo vascularization [24, 25].

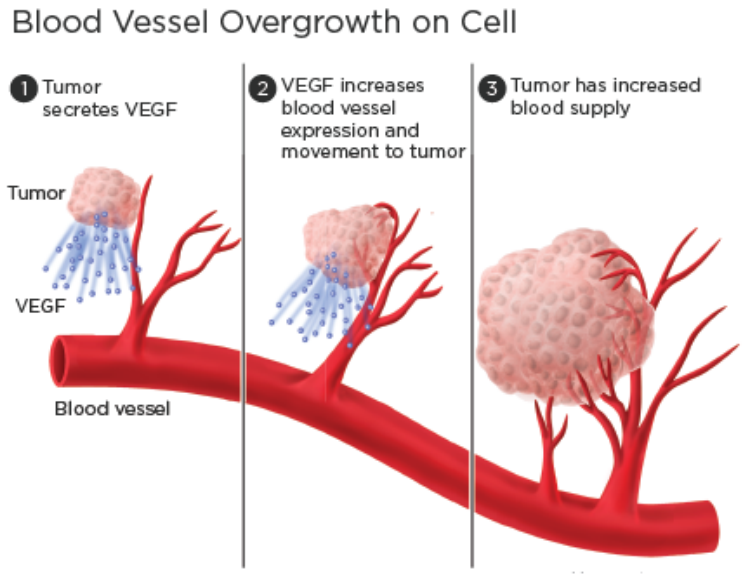


**Figure 2.1**: Neo-vascularization

Figure 2.1 shows increase in size of tumor after new vascular supply. VEGF disrupts vascular network ultimately causing sprouting of existing blood supply towards the tumor.

Hahnfeldt [9] proposed a model which is primarily accountable for illustrating dynamic nature of carrying capacity and usefulness of anti-angiogenic drugs. As introduced earlier, angiogenesis is a physiological process through which new blood vessels are formed from the pre-existing vessels. Tumors need a dedicated blood supply to provide the oxygen and other essential nutrients in order to grow beyond a certain size (1-2 $mm^2$). Tumors induce blood vessel growth i.e. angiogenesis, by secreting various growth factors. Angiogenic features are considered key to the differentiation between low and high grade gliomas [10].

Mitogen and VEGF are the main types of protein found to be present in the hypoxic (oxygen-deprived) tumor cells which lies adjacent to necrotic (quiescent) region [10]. Mitogen encourages a cell to commence cell division whereas VEGF is a signal protein which stimulates angiogenesis by creating a chemical gradient. The chemical gradi-

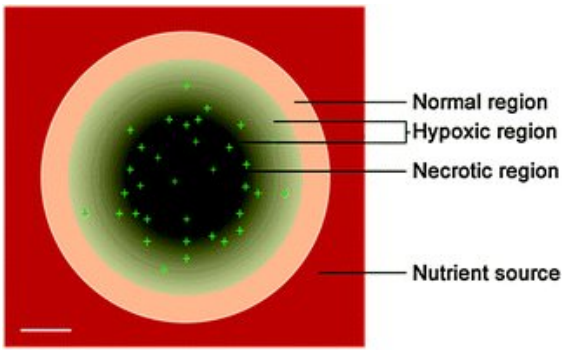


**Figure 2.2**: Proliferative, hypoxic and necrotic region of a tumor spheroid [16]

ent triggers endothelial cells (EC) in the pre-existing vasculature to migrate towards the tumor. Eventually, an accumulation of ECs forms a finger-like capillary sprout extending from parent vessels.

Figure 2.2 shows three major regions of a tumor spheroid. Inflow of vital nutrients (particularly oxygen) is caused by the diffusion, which is however, a slow process. Due to this cell proliferation eventually only takes place near the surface (normal region) of the tumor where the nutrient level is sufficiently high. Deeper inside the tumor nutrients level drop significantly due to which the cells belonging to middle ring, hypoxic region, remain quiescent. They become actively proliferating again once there is an enough nutrient supply for example, by angiogenesis. Deeper yet (innermost, necrotic), the nutrient level is almost negligible that the tumor cells begin to die. Most of the cells belonging to this region are dead.

It has also been agreed that the tumor itself produces smaller amounts of angiogenic inhibitor (mostly angiostatin, a naturally occurring or an endogenous protein) along with the production of large amount of stimulator [24, 25]. For a dormant (relatively stable or very slowly growing) tumor, there is a balance between angiogenic inhibitor and stimulator produced by tumor itself ( Tumor never grows hypothesis). Hahnfeldt's [9] model incorporates anti-angiogenic drugs like angiostatin in one dimensional tumor growth model of tumor volume (assuming Gompertzian growth) and

carrying capacity (which no longer remains static after angiogenesis). As proposed by Hahnfeldt [9], following two, one dimensional models represent temporal evolution of tumor volume and dynamic carrying capacity:

$$\frac{dV(t)}{dt} = -\lambda V \log \frac{V(t)}{K(t)} \tag{2.4}$$

$$\frac{dK(t)}{dt} = bV(t) - dK(t)V(t)^{\frac{2}{3}} - eK(t)g(t) \tag{2.5}$$

where,V is the tumor volume ($mm^3$) and K is dynamic carrying capacity ($mm^3$).$\lambda$ (1/day), b (1/day), d (1/day), and e (1/day) are the control parameters (assumed to be constant) and

$$g(t) = \int_0^t c(t')e^{-\mathrm{clr}(t-t')}dt' \tag{2.6}$$

is the concentration of administered anti-angiogenic drug c(t′) rate of administration clr is the clearance rate (1/day) of previously administered drug.

First term i.e. bV(t) in Eq. (2.6) is stimulation capacity (assumed to be acting locally to the individual tumor secreting site) due to simulators like VEGF produced by tumor itself. Based on the Eq. (2.5), this term increases tumor capacity rate.

Second term i.e. $dK(t)V(t)^{\frac{2}{3}}$ represent inhibitory effect (effect of endogenous inhibitor like angiostatin on vasculature, produced by tumor itself) and is assumed to be acting on surface only. This term lowers tumor capacity expansion rate.

And third term represents inhibition of tumor vasculature due to administered inhibitor with concentration g(t) [9].

The significance of the Hahnfeldt model is that simulators and inhibitors produced by tumor are responsible for the change in tumor carrying capacity and which, ultimately, provides more room for the growing tumor. The tumor remains isolated and fixed as long as carrying capacity does not change, and this phenomenon is called tumor dormancy (Tumor never grows hypothesis).

## 2.2 PARTIAL DIFFERENTIAL EQUATIONS

### 2.2.1 Reaction-Diffusion Model

Reaction-diffusion model of Murray [12] is based on the exponential growth of reaction term (proliferation of cells) and migration of cells due to passive diffusion (Fickian):

$$\frac{\partial c(x,t)}{\partial t} = \nabla[D(x)\,\nabla\, c(x,t)] + \rho\, c \tag{2.7}$$

where, c(x,t ) represents number density (cells/mm$^3$) with spatio-temporal dependence, $1^{st}$ term in right hand side accounts for diffusion with D(x) being diffusion coefficient (mm$^2$/day) and $2^{nd}$ term represents proliferation (exponential growth) with $\rho$ describing net proliferation rate (1/day). The diffusion coefficient in above equation has spatial dependence while proliferation rate is independent of spatial variation.

Diffusion coefficient varies in a very different way in the case of white matter (WM), gray matter (GM), and cerebrospinal fluid (CSF) which constitute most of the brain architecture. Especially, diffusion of tumor cells in white matter is highly anisotropic compared to gray matter and this trend of heterogeneity pattern of diffusion of tumor cells is very similar to water flow inside the brain.

As a consequence of limited availability of nutrients and space, exponential growth pattern of tumor cell density c(x,t), however, no longer remains relevant. Rockne [11] modified this equation by assuming logistic growth. Same variation of radiotherapy killing rate (with logistic growth) was proposed after Rockne incorporated linear quadratic (LQ) model of cell survival in reaction-diffusion model:

$$\frac{\partial c(x,t)}{\partial t} = \nabla[D\,\nabla\, c(x,t)] + (\rho\, - R)c\left(1 - \frac{c}{K}\right) \tag{2.8}$$

where, K called carrying capacity (cells/mm$^3$) of the tissue, is equal to tumor density when net proliferation is saturated (unless it is triggered by angiogenesis). Other parameters represent same information as mentioned in Eq. (2.7). R is radiation killing fraction defined below

$$R(\alpha, D(x,t)) = \begin{cases} 0 & \text{for no therapy} \\ 1 - \mathrm{S}(\alpha, \beta, \mathrm{D(x,t)}) & \text{for therapy} \end{cases} \tag{2.9}$$

where, D(x,t) is the radiation dose (Gy) distribution and S is the estimated surviving fraction using the Linear Quadratic (LQ) cell survival model with the parameters $\alpha$ (1/Gy) and $\beta$ (1/Gy$^2$).

Using linear-quadratic (LQ) radiation dose-response model:

$$S = e^{(-\alpha d(x,t) - \frac{\beta}{n} d(x,t)^2)} \tag{2.10}$$

with,

$$D(x,t) = n\, d(x,t) \tag{2.11}$$

where, d(x,t) and n represent fractionated dose and the number of fraction respectively.

Eq. (2.10) can be modified as:

$$S = e^{-\alpha(d(x,t) - \frac{1}{n(\frac{\alpha}{\beta})} d(x,t)^2)} \tag{2.12}$$

where, the ratio $\frac{\alpha}{\beta}$ represents the tissue response. For early effects (actively proliferating glioblastoma tumor cells), $\frac{\alpha}{\beta}$ is large ($\approx$10Gy), thus $\alpha$ dominates surviving fraction at small doses while $\beta$ dominates for late responding cases [30]. Similarly, n and d(x,t) are respective values of number of fractions and dose per fraction in the case of fractionated radiotherapy treatment modality.

In the context of actively proliferating cells like glioma cells, the factor $\alpha$, called radio sensitivity parameter, is main indicator of quality of the radiotherapy treatment. With parameters n and d(x,t) fixed in Eq. (2.10), survival and hence killing rate primarily depend on the choice of the parameter $\alpha$.

In the absence of radiotherapy term, Eq. (2.8) can be reduced to the classic Fisher-Kolomorov equation. The equation has an analytical solution in the case of homoge-

neous diffusion ('Traveling wave approximation' [11]):

$$\frac{\partial c(x,t)}{\partial t} = \frac{\partial^2 c(x,t)}{\partial x^2} + \rho\, c(x,t)\left(1 - \frac{c(x,t)}{K}\right) \tag{2.13}$$

If a traveling wave solution exists of the form c(x, t) = C(z) where,

$$z = x - vt$$

with the speed of tumor isodensity (boundaries are assumed to have same density values) wavefront v ($> 0$), then velocity [11] is given by

$$v \geq 2\sqrt{D\rho}$$

And the minimum speed (Fisher approximation, [11]) is given by

$$v = 2\sqrt{D\rho} \tag{2.14}$$

Main aspects of Swanson model (Eq. (2.8)) is that net proliferation rate $\rho$ and diffusion coefficient D can describe actual tumor density growth if initial tumor density value is known. Important qualitative aspects of tumor whether it is actively proliferating or diffusion dominated ('Grow or go hypothesis') can be interpreted in terms of invisibility index,$\lambda$ (=D/$\rho$):

1. Higher value of $\lambda$ indicates that tumor evolution is diffusion dominated. This is the situation where the tumor is spreading and invading nearby tissues possibly indicating its phase after vascularization (angiogenesis). Higher diffusion coefficient value also points out that diffusion is preferentially along the white matter.

2. Lower value of $\lambda$ indicates tumor remained in its earlier phase (avascular) where only proliferation is the dominating factor.

### 2.2.2 Patient Specific Model Parameters D and $\rho$

The boundary of the hyperdense angiogenic tissue and necrotic regions are detected by T1Gd while the boundary of the edema (swelling part around tumor) is detected

by the T2-FLAIR ( Figure 2.8). T1Gd and T2-FLAIR are the imaging classes of magnetic resonance imaging (MRI) modality with the characteristics explained in the Section 2.3.

The equivalent tumor volumes for T1Gd and T2-FLAIR extracted from three dimensional segmentation of respective images are translated to a spherically-equivalent radius by

$$r = \left(\frac{3V}{4\pi}\right)^{\frac{1}{3}}$$

Radius of T1Gd and T2-FLAIR isodensity wavefront are represented by $r_{T1Gd}$ and $r_{T2}$ respectively. After calculating respective radii from images (of same modality i.e. either T1Gd or T2-FLAIR) at two different time points, velocity can be computed using following formula:

$$v_{T1Gd,T2} = \frac{r^2_{T1Gd,\ T2} - r^1_{T1Gd,T2}}{t_2 - t_1} \tag{2.15}$$

Thus calculated image based velocity is equal to $2\sqrt{D\rho}$ as given in Eq. (2.14) and this is relevant only when tumor has grown significantly in large time [11]. There needs to be significant amount of accumulation of tumor cells before they become visible in MRI. According to [20] , images become detectable only when tumor density reaches $8000/mm^3$ indicating there has already been significant lapse of time.

Invisibility index ($\lambda = \frac{\rho}{D}$) is another quantity which can be measured using T1Gd and T2-FLAIR and with the velocity formula (Eq. (2.15)), patient specific $\rho$ and D can be obtained [11].

Boundaries of T1Gd and T2-FLAIR are characterized by same tumor density values and thus refereed as isodensity line. Rockne [11] has proposed isodensity values corresponding to T1Gd and T2 enhanced boundaries equal to 0.8 and 0.16 of carrying capacity K respectively.

Figure 2.3 shows three major regions of glioblastoma recorded by MRI. Central portion represents solid tumor which mainly consists of necrotic cells. Tumor cell density

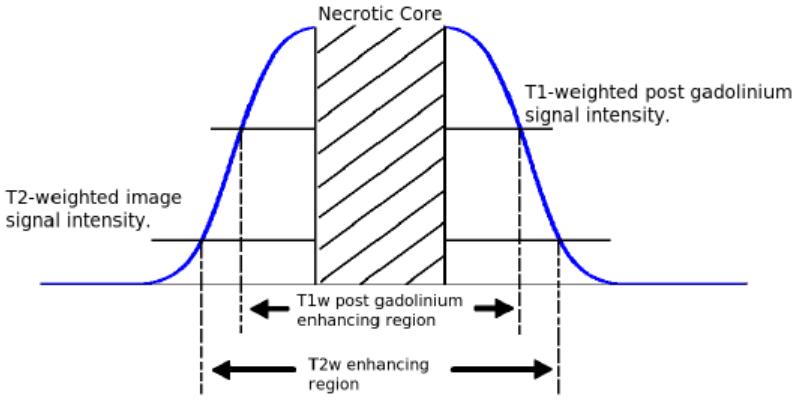


**Figure 2.3**: Necrotic,T1Gd and T2-FLAIR enhancing regions [19].

remains uniform in this region. First fall-off portion which is detected by T1Gd image mainly consists of actively proliferating cells (caused by angiogenesis) while second fall-off region includes edematous region which is accounted by T2-FLAIR to some extent. However there is finite amount of tumor cells escaping even from T2-FLAIR boundary shown by the tail of the curve in either side.

### 2.2.3 Reaction-Convection Model

Another approach describing tumor development in brain is reaction-convection based model [13]. In the context of this research this model represents the tumor regrowth after surgery.

Cell proliferation and cell death induce changes in the tumor volume [8]. To be more precise, there is a movement of cells within the tumor due to proliferation and removal (due to necrosis) [13]. As a result, a convection terms appears (for mass conservation) that accounts for both diffusion (due to random motion in individual cell level) and advection (due to bulk flow that involves the entire cells). Mathematical modeling of reaction-convection equation assumes a spherical tumor (spheroid) regrowth, after

resection with further assumption of radially symmetry. Following equations are proposed by taking account of convection term in conservation of mass of tumor cells and necrotic cells:

$$\frac{\partial x(r,t)}{\partial t} + \frac{1}{r^2}\frac{\partial}{\partial r}[r^2 u(r,t)x(r,t)] = \lambda\, x(r,t) - \delta\, x(r,t) \tag{2.16}$$

$$\frac{\partial y(r,t)}{\partial t} + \frac{1}{r^2}\frac{\partial}{\partial r}[r^2 u(r,t)y(r,t)] = \delta\, x(r,t) - \mu\, y(r,t) \tag{2.17}$$

where, x(r,t) and y(r,t) are number density of tumor and dead cells respectively. u(r,t) is radial velocity, assumed to be same for both the tumor and dead cells. Constant terms $\lambda$, $\delta$ and $\mu$ refer to proliferation rate of tumor cells, rate of necrosis, and rate of removal of cells from regrown tumor into fluid (occupied in resected part) respectively. The effect of radiotherapy and chemotherapy can be observed by introducing respective killing rate in Eqs. (2.16) and (2.17) as

$$\frac{\partial x(r,t)}{\partial t} + \frac{1}{r^2}\frac{\partial}{\partial r}[r^2 u(r,t)x(r,t)] = (\lambda\ - \delta\ - A\rho(t) - B\tau(t))x(r,t) \tag{2.18}$$

$$\frac{\partial y(r,t)}{\partial t} + \frac{1}{r^2}\frac{\partial}{\partial r}[r^2 u(r,t)y(r,t)] = (\delta\ + A\rho(t) + B\tau(t))x(r,t) - \mu y(r,t) \tag{2.19}$$

where, A$\rho(t)$ and B$\tau(t)$ are respective radiotherapy and chemotherapy killing rate. The parameter A is same as radiation killing rate R defined in Eq. (2.9) and Eq. (2.10) of reaction-diffusion model [11].

## 2.3 CURRENT CLINICAL PRACTICES FOR THE TREATMENT OF GLIOBLASTOMA AND CHALLENGES

The standard treatment for newly diagnosed glioblastoma multiforme is surgical resection followed by radiotherapy and chemotherapy. Magnetic resonance imaging (MRI) is performed for the diagnosis as well as for the follow up using its T1Gd

and T2-FLAIR modalities. Gadolinium (Gd) is used as contrast enhancing agent in T1 weighted MRI due to its paramagnetic (two unpaired electrons in valance cell)and non-toxic nature. It preferentially attaches with the area of active tumor growth,where new blood vessels are created (angiogenic). Thus, angiogenic areas surrounding central necrotic region becomes hyperintense while middle portion appears hypointense. Due to this fact, T1Gd region correlate with high tumor cell density and 'bulk tumor'. T2-FLAIR (Fluid-Attenuated-Inversion Recovery) is similar to a T2-weighted image; except that repetition time (TR) and echo time (TE) are very large. By doing so, CSF is not enhanced as in the T2-weighted image. Thus, nearby pathologies close to CSF can be better visualized [19]. Currently, standard- of -care for radiotherapy consists of conformal radiation delivery (30 daily fractions of 2 Gy for a total of 60 Gy) to the bulk tumor plus an isotropic 2-3 cm margin to include infiltrative tumor area [14]. Radiotherapy planning is typically based on the bulk tumor also called gross tumor volume (GTV) which is visible portion of T1Gd. Infiltrative region, which can be seen to some extent in T2- FLAIR, is taken into account by expanding GTV isotropically around 2-3 cm. This region is called clinical target volume (CTV) through which homogeneous radiation of 63 Gy is delivered in 35 fraction as stated above. This approach results in dose plans that are spatially uniform over the target volume, however, do not account for patient-specific biological heterogeneity up to the optimal extent [14].

Figure 2.4 displays different imaging modalities for the diagnosis of glioblastoma. Three images in first row are three different MRI imaging classes discussed in Section 2.2.2. These image classes are currently in practice. Fractional anisotropy (FA) and mean diffusivity (MD) are the imaging classes of diffusion tensor imaging (DTI). FA and MD imaging modalities are looking promising as tumor diffusion pattern in brain vastly resembles with diffusion of water. However, these modalities are not being used

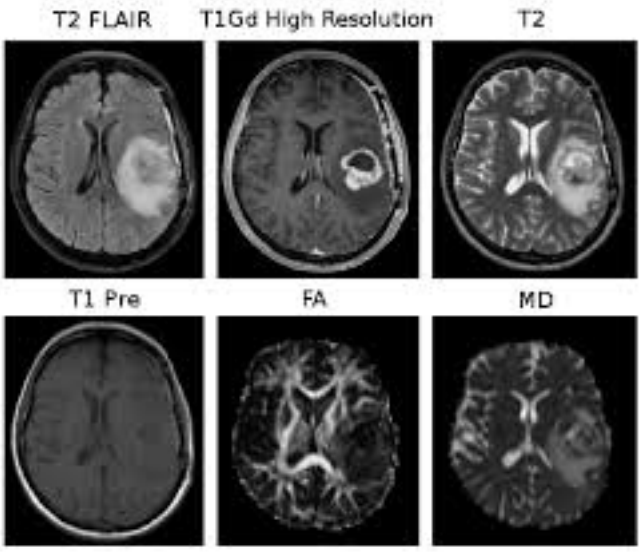


**Figure 2.4**: Various MRI modalities used in diagnosis of glioblastoma [15].

.

extensively in clinics due to poor contrast issue and lengthy image acquisition time. Patient specific parameters, net proliferation rate and diffusion coefficient, are obtained from T1Gd and T2-FLAIR using Eq. (2.14) and invisibility index. These values can be incorporated into mathematical model given by Eqs. (2.8) and (2.18) so that simulation result can predict true tumor growth pattern as in vivo, and the treatment plan (radiotherapy and chemotherapy) can be designed accordingly.

However, challenges still remain significant as invasion of tumor cells still can not be covered by above imaging modalities (T1Gd and T2-FLAIR) fully due to preferential and highly diffuse pattern along white matter. Usefulness of functional imaging modalities like amino acid Positron Emission Tomography (PET), including FET (Fluoro-Ethyl-Tyrosine) MET (Mehionine) has been suggested as an alternative of MRI [17]. However, these PET modalities have also poor contrast issue in the area of low tumor cells infiltration [17]. Mathematical modeling given in Eq. (2.8) requires precise information about initial tumor density profile (assuming patient specific pa-

rameters, $\rho$ and D calculated on the same day images taken) to predict its future value. As stated in section 2.2.2 and also in [18], boundaries of T1Gd volume corresponds to an isoline of the tumor cell density (0.8 of K assumed in [18] also in [11]). This boundary serves as starting point for the tumor cell density. The tumor cell density is then extrapolated into the brain, and, also the anatomical constraints (glioma does not infiltrate falx cerebri and ventricles) in the brain tissue segmentation (Figure 2.5) are taken into account. Based on the actual tumor density profile (Figure 2.6), the target volume (Figure 2.7) can be delineated and radiation dose is then prescribed accordingly [18]. Fall-off portion (outside T2-FLAIR) in Figure 2.3 remains challenging so far as it has been not possible to be included in dose profile very precisely. As suggested in [18] tumor density varies exponentially with the distance ($|r|$) from the visible tumor. The following relation has been proposed:

$$c(|r|) \propto e^{(-|r|/\lambda_w)} \tag{2.20}$$

where $\lambda_w$ , infiltration length, is the distance at which cell density drops by a factor of $e$ in white matter. And it is related to model parameters D and $\rho$ (discussed in Section 2.2.2) by the following relation:

$$\lambda_w = \sqrt{\frac{D_w}{\rho}} \tag{2.21}$$

Similar relations can be expected for the gray matter. Tumor cell density calculated using above step can be implemented for target volume delineation [18].

Figure 2.8 shows the systematic scheme for the calculation of patient specific parameters, net proliferation rate ($\rho$) and diffusion coefficient (D) based on the patient image data. Tumor radii of T1Gd and T2-FLAIR images are calculated from the equivalent sphere of the respective 3D tumor volume. After then velocity is computed. Invisibility index is also calculated using two different imaging classes taken at the same time. Diffusion coefficient and net proliferation are finally calculated using formula described in Section 2.2.2.

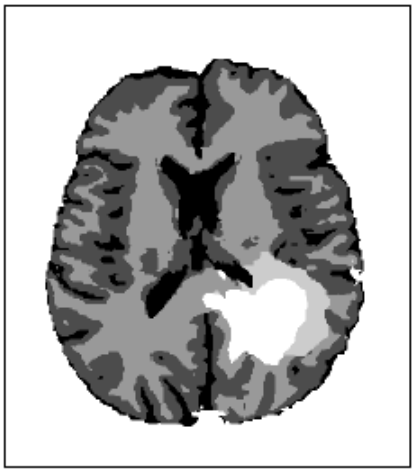

**Figure 2.5**: Segmentation of the brain into contrast enhancing core (white),T2-FLAIR boundary (light white), white matter (light gray), gray matter (dark gray), and CSF (black) [18].

.

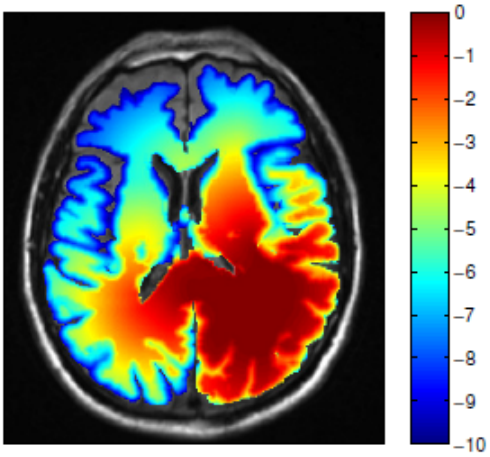


**Figure 2.6**: Cell density based on brain segmentation in Figure 2.5 [18].

.

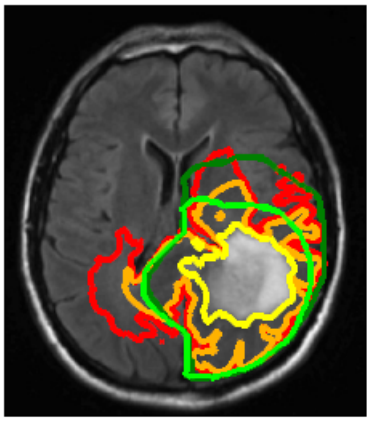

**Figure 2.7**: Comparison of manually defined targets (light/dark green) and model based targets (red/yellow). Light green contour represents boundary of T2-FLAIR with isotropic margin while dark green is PTV [18].

## 2.4 SCOPE OF PRESENT WORK

Undoubtedly, mathematical modeling has great impact on the clinical treatment of glioma including its most aggressive form glioblastoma multiforme (GBM). Knowledge of the actual initial tumor density profile and then its brain-segmentation based temporal evolution are only gained through mathematical modeling. Once tumor density is calculated, target volume can be delineated and treatment plan can then be set accordingly. Besides above point, mathematical modeling can also incorporate different types of active migration processes like chemotaxis along with the passive diffusion component in either reaction-convection or diffusion model described in previous section. Target volume delineation also makes remarkable progress if it is aided by imaging modalities like diffusion tensor imaging which can track tumor cells in the individual level by monitoring actual diffusion process occurring inside brain. Diffusion tensor imaging again relies on mathematics for the various applications like image registration, image distortion minimization by linear and non-linear registration of images etc.

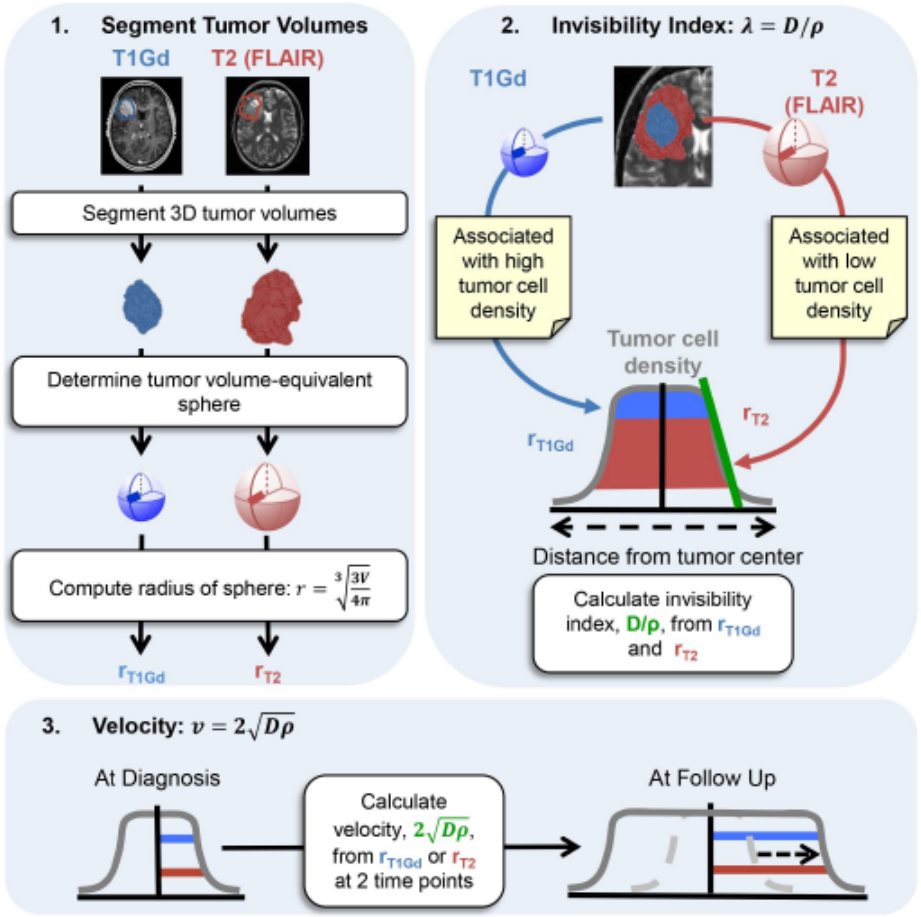


**Figure 2.8**: Calculation of diffusion coefficient and net proliferation rate from patient specific MRI scan [14].

Based on the importance of mathematical modeling, this research attempts to validate various glioma growth models given in the form of differential equations numerically. In the first part, non-linear partial differential equations proposed by Tian [13] is solved in which all three standard treatment schemes, resection, radiotherapy, and chemotherapy for the treatment of glioblastoma multiforme (GBM) are implemented. This work also attempt to see effects of radio sensitivity parameter, $\alpha$, alpha-beta ratio ($\frac{\alpha}{\beta}$) of linear quadratic model in the radiotherapy treatment after resection.

Constant parameter, initial values, and boundary values are all adapted from the same paper. This work uses basic numerical schemes like forward Euler's, forward time centered space (FTCS) in spherical coordinates with radial symmetry which is always reasonable as the shape of tumor resembles with the spheroid, and most of the mathematical models are based on tumor spheroid.

Numerical solution of the Swanson's equation [11] will also be performed in spherically symmetric case using clinically measured values of diffusion coefficient (assuming homogeneous diffusion) and net proliferation rate. Future evolution of tumor cell density can be estimated and compared with in vivo growth if its initial value is precisely known. It is widely accepted that there is already significant level of diffusion process that has occurred during the diagnosis (There is minimum threshold of detection of imaging modalities like MRI). Initial condition of tumor cell density is taken as Gaussian initial tumor profile as suggested in [21] assuming diffusion process has already taken place.

Tumor density profiles respective to the diffusion coefficient values of white matter and gray matter will be compared. The difference can necessarily bring the issue to address inhomogeneity of the brain in mathematical calculation so that the result can be incorporated in vivo. Similar comparison can be made by using two different values of net proliferation rate while keeping diffusion coefficient the same, and it will

highlight proliferation dominated tumor growth in its early phase.By incorporating radiotherapy (Eq. (2.8)), effects (similar approach as in the Eq. (2.10)) of various linear quadratic model parameters of the cell survival equation (Eq. 2.10) on the tumor density profile can be observed.

Tumor growth model under angiogenic therapy [9] mentioned in Eq. (2.5) and Eq. (2.4) is also solved numerically using parameter values used in [9]. Anti-angiogenic drugs are non-cell killing (cytostatic) drugs. They only block angiogenic growth factors like VEGF being secreted by tumor. However, due to blockage of neo vascularization and nutrients, tumor remains dormant and eventually die without damaging normal tissue composition. Tumor volume and carrying capacity growth rate under angiogenic inhibitors and simulators will be shown. The effect of anti-angiogenic drugs (artificial inhibitors) on the mathematical model will also be dealt. The various parameter values are taken from [9].

Numerical solution of all differential equation modalities discussed above and in Chapter 2, is done in MATLAB R2015b (The MathWorks, Inc., Natick, Massachusetts, United States).

Outcome of numerical solution is given in 'Result and Discussion' section with relevant Matlab scripts in 'Appendix'.

# CHAPTER 3

# METHODS

## 3.1 NUMERICAL METHODS FOR DIFFERENTIAL EQUATIONS

Taylor expansion of any function y=f(x) around h is given by,

$$y_1 = f(x+h) = f(x) + h\frac{df}{dx} + \frac{h^2}{2}\frac{d^2f}{dx^2} + ... \tag{3.1}$$

Similarly, around -h,

$$y_{-1} = f(x-h) = f(x) - h\frac{df}{dx} + \frac{h^2}{2}\frac{d^2f}{dx^2} + ... \tag{3.2}$$

From Eq. (3.1)

$$\frac{df}{dx} \approx \frac{f(x+h) - f(x)}{h} + \mathrm{O(h)} \tag{3.3}$$

where, O(h) is an error function proportional to h. In general, for

$$\begin{aligned} x(i) =& i\,dx, i = 1, 2, ..., M+1 \\ \text{with}\, dx =& \frac{L}{M+1},\ x(1) = 0\ x(M+1) = L \end{aligned} \tag{3.4}$$

$$\frac{dy}{dx}\Big|_{x_i} \approx \frac{y(i+1) - y(i)}{dx} + \mathrm{O(dx)}, \qquad \text{with}\, dx = h \qquad \text{Euler's forward difference} \tag{3.5}$$

Adding Eq.(3.1) and Eq.(3.2)

$$\frac{d^2f}{dx^2} \approx \frac{(f(x+h) - 2\,f(x) + f(x-h))}{h^2} + O(h^2) \tag{3.6}$$

In the discretization scheme:

$$\frac{d^2y}{dx^2}\Big|_{x_i} \approx \frac{(y(i+1) - 2\,y(i) + y(i-1))}{dx^2} + O(dx^2), \text{ with}\, dx = h \,\text{Central difference} \tag{3.7}$$

Also,(subtracting Eq. (3.1) and Eq. (3.2))

$$\frac{dy}{dx}\Big|_{x_i} \approx \frac{y(i+1) - y(i-1)}{2\,dx} \qquad \text{Central difference} \tag{3.8}$$

These basic numerical scheme can be extended for any kinds of partial differential equation. For example, Diffusion equation in one dimension (with no reaction term):

$$\frac{\partial u}{\partial t} = D\,\frac{\partial^2 u}{\partial x^2} \qquad \text{with}\, u = u(x,t) \tag{3.9}$$

can be solved using forward difference in time and the central difference in space also called FTCS scheme.

For

$$\begin{aligned} x(i) =& i\,dx, i = 1, 2, ..., M+1 \\ \text{with}\, dx =& \frac{L}{M+1},\; x(1) = 0\,,\; x(M+1) = L \end{aligned} \tag{3.10}$$

And

$$\begin{aligned} t(n) =& n\,dt, n = 1, 2, ..., N+1 \\ \text{with}\, dt =& \frac{T}{N+1},\; t(1) = 0\,,\; t(N+1) = T \end{aligned} \tag{3.11}$$

Forward difference in time:

$$\frac{\partial u}{\partial t}\Big|_{x_n,t_n} \approx \frac{u(i,n+1) - u(i,n)}{dt} + O(dt) \tag{3.12}$$

Similarly, central difference in space:

$$\frac{\partial^2 u}{\partial x^2}\Big|_{x_n,t_n} \approx \frac{u(i+1,n) - 2\,u(i,n) + u(i-1,n)}{dx^2} + O(dx^2) \tag{3.13}$$

Complete numerical scheme for the temporal evolution of parameter u(x,t) can be obtained by substituting values obtained from Eq. (3.12) and Eq. (3.13) into Eq. (3.9).

$$u(i,n+1) \approx u(i,n) + \frac{D\,dt}{dx^2}\;(u(i+1,n) - 2\,u(i,n) + u(i,n-1)) \tag{3.14}$$

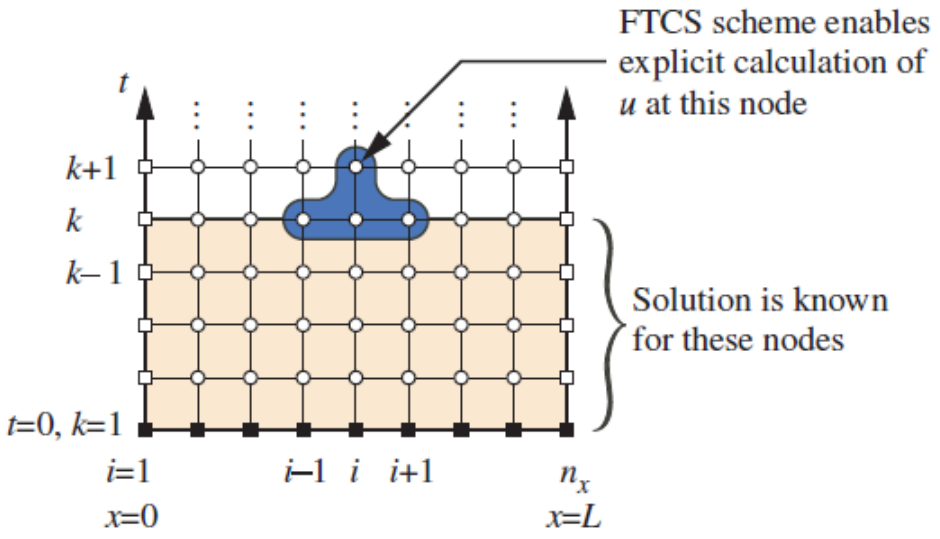


**Figure 3.1**: The stencil for FTCS scheme

The parameter,

$$K = \frac{D\,dt}{dx^2}$$

determines the stability of numerical method (FTCS) of partial differential equation Eq. (3.9).

$$K \leq \frac{1}{2}$$

is the stability criteria for the numerical solution of Eq. (3.9) (Von Neumann stability criteria). Time step (dt) and radial distance step (dr) in numerical solution of reaction-diffusion model given in Eq. (3.46) are adjusted with the experimentally measured value of diffusion coefficient, D, to meet above stability criteria. However, Voe Neumann stability criteria given above simply does not hold correct for the non-linear hyperbolic partial differential equation of type (Eq. (3.15) and Eq. (3.19)).

Figure 3.1 shows FTCS scheme. This scheme uses values of u at previous time level k ( u(i+1,k), u(i-1,k) and u(i,k)) to calculate its value of next time label k+1 (u(i,k+1)).

## 3.2 REACTION-CONVECTION MODEL

### 3.2.1 Scaling and Transformation

The standard treatment for newly diagnosed glioblastoma multiforme is surgical resection followed by radiotherapy and chemotherapy. This research is focused on validating outcome of [13] by solving partial differential equations Eq. (2.18) and Eq. (2.19) using simple numerical approach. There is a similar outcome in [22] where partial differential equation are converted into ordinary differential equation by ignoring spatial dependence of tumor cells density. Direct numerical solution of non-linear hyperbolic partial equations given in [13] preserves spatio-temporal dependence of tumor cell density, of which analytical solution is very hard to achieve. Forward time and centered space (FTCS) scheme is used to solve these equations. Rewriting Eq. (2.16) and Eq. (2.17):

$$\frac{\partial x(r,t)}{\partial t} + \frac{1}{r^2}\frac{\partial}{\partial r}[r^2 u(r,t)x(r,t)] = \lambda\, x(r,t) - \delta\, x(r,t) \tag{3.15}$$

$$\frac{\partial y(r,t)}{\partial t} + \frac{1}{r^2}\frac{\partial}{\partial r}[r^2 u(r,t)y(r,t)] = \delta\, x(r,t) - \mu\, y(r,t) \tag{3.16}$$

The equations represent tumor/necrotic cells density (cells/mm$^3$) dynamics without including radiotherapy and chemotherapy.

According to [13] the standard radiotherapy treatment consists of fractionated irradiation at a dose of 2 Gy per fraction given daily, 5 days per week (Monday through Friday), over a period of 6 weeks, for a total dose of 60 Gy. Similarly, chemotherapy dosing scheme consists of temozolomide (FDA approved drug with brand names Temodal or Temcad) at a dose of 75 mg per square meter of body surface per day, given 7 days a week from the first day of radiation until the last day of radiation.

Then, after a 4-weeks break, chemotherapy continues, and patients receive a double dose of temozolomide for 28 days (4 weeks). After the end of this period, another cycle of temozolomide dose is administered at 8/3 level of the original dose.

Based on the above schemes, radiotherapy activity function ($\rho(t)$) and chemotherapy dosing function ($\tau(t)$) are defined as:

$$\rho(t) = \begin{cases} 1 & \text{if } 6 \leq t \leq 12 \\ 0 & \text{otherwise} \end{cases} \tag{3.17}$$

$$\tau(t) = \begin{cases} 1 & \text{if } 6 \leq t \leq 12 \\ 2 & \text{if } 16 \leq t \leq 20 \\ \frac{8}{3} & \text{if } 20 \leq t \leq 40 \\ 0 & \text{otherwise} \end{cases} \tag{3.18}$$

The rate by which radiotherapy kills tumor cells is given by a parameter A(1/week). Thus, product of A and $\rho(t)$ i.e. $A\rho(t)$ gives death rate by radiotherapy. Similarly the product $B\tau(t)$ gives killing rate by chemotherapy treatment with parameter B(1/week) chemotherapy killing rate. To follow standard treatment scheme, both killing rates can be incorporated in Eq. (3.15) such that

$$\frac{\partial x(r,t)}{\partial t} + \frac{1}{r^2}\frac{\partial}{\partial r}[r^2 u(r,t)x(r,t)] = (\lambda\ -\delta\ - A\rho(t) - B\tau(t))x(r,t) \tag{3.19}$$

represents tumor cell density x(r,t) evolution.

Eq. (3.15) can be further simplified as:

$$\frac{\partial x(r,t)}{\partial t} + \frac{1}{r^2}\frac{\partial}{\partial r}[r^2 u(r,t)x(r,t)] = \alpha(t)x(r,t). \tag{3.20}$$

where,

$$\alpha(t) = (\lambda\ -\delta\ - A\rho(t) - B\tau(t) \text{ and } x'(r,t) = \frac{x(r,t)}{\theta} \tag{3.21}$$

x′(r,t) is replaced by x(r,t) for further calculation for simplicity.

As mentioned in Section 2.2.3, radiotherapy killing parameter A is related to linear quadratic model (Eq. (2.10)) as:

$$A = 1 - e^{(-\alpha d(x,t) - \frac{\beta}{n} d(x,t)^2)} \tag{3.22}$$

For fractionated radiotherapy scheme (with fixed number of fractions and dose per fraction), value of A can be substituted in Eq. (3.21) so that tumor density can be computed for various value of radio sensitivity parameter, $\alpha$. Similar approach can be implemented for early and late responding tissues (variable alpha-beta ratio).

Similarly, the following equation

$$\frac{\partial y(r,t)}{\partial t} + \frac{1}{r^2}\frac{\partial}{\partial r}[r^2 u(r,t) y(r,t)] = (\delta \ + A\rho(t) + B\tau(t))x(r,t) - \mu y(r,t) \tag{3.23}$$

represents necrotic cells density dynamics under radiotherapy and chemotherapy. For this work, only tumor cells density dynamics given in Eq. (3.19) is of interest.

Some assumptions are made before solving these partial differential equations numerically [13]:

1. There is a radially symmetric growth of tumor such that boundary of tumor can be represented by

$$r = R(t). \tag{3.24}$$

The time evolution of tumor radius is essentially free boundary problem which makes numerical solution difficult to achieve. To solve this problem, moving boundary is mapped into a fixed one by introducing a new coordinate (Landau transformation [23]).

2. Total density of tumor and necrotic cells is constant through the tumor i.e.

$$x(r,t) + y(r,t) = \text{constant}(\theta) \tag{3.25}$$

which is equal to $10^6/\text{mm}^3$.

3. Tumor does not grow inward that is u($R^*$,t)=0, where $R^*$ is radius of resected

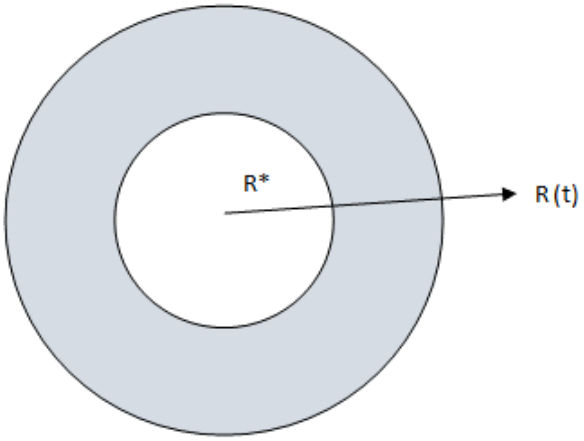


**Figure 3.2**: Resected spherical tumor

tumor.

Figure 3.2 is a simple sketch of resected and active spherical tumor.Innermost sphere with radius $R^*$ is the portion of tumor resected. Outer surface of the proliferating cells is represented by a growing radius R(t). Necrotic and dead cells pushed towards inner core are washed out by CSF, which fills empty part of resected tumor.

Values of various parameters including constants are chosen same as those used in [13]. A value of 20 mm refers to radius of totally resected tumor [13] , [26]. A slightly smaller value of radius $R^*$=18 mm is chosen to observe effect of partial resection on the tumor survival time.

Table 3.1 gives the values of various model parameters used in [13]. The difference of proliferation rate of tumor cells and rate of necrosis given here is equivalent to the net proliferation rate ($\rho$) used in reaction-diffusion model [11]. Similarly, radiotherapy killing rate A is equal to the radiation killing fraction, R given in Eq. (2.9) and Eq. (2.10).

Equation for the radial velocity u(r,t) can be obtained by adding Eq. (3.19) and Eq.

**Table 3.1**: Reaction-convection model parameters values

| Parameters | Description | Numerical values | Dimensions |
|---|---|---|---|
| $\lambda$ | Proliferation rate of tumor cells | $2 \times 10^{-2}$ | 1/hour |
| $\delta$ | Rate of necrosis | $1.89 \times 10^{-2}$ | 1/hour |
| A | Radiation killing rate | 1.01 | 1/hour |
| $\mu$ | Removal rate of necrotic cells | $\frac{1}{72}$ | 1/hour |
| B | Temozolomide killing rate | 0.03 | 1/hour |

(3.23)

$$\frac{1}{r^2}\frac{\partial}{\partial r}[r^2 u(r,t)] = F \tag{3.26}$$

where,

$$F = \beta\, x(r,t) - \mu \qquad \text{and} \qquad \beta = \lambda + \mu$$

First boundary condition:

$$u(R^*, t) = 0 \tag{3.27}$$

Tumor radius evolves according to (moving boundary condition):

$$\frac{dR(t)}{dt} = u(R(t), t) \tag{3.28}$$

Now using Eq. (3.23) and Eq. (3.26)

$$\frac{\partial x}{\partial t} + u(r,t)\frac{\partial x}{\partial r} = \beta x(r,t)\left(\frac{\alpha+\mu}{\beta} - x(r,t)\right) = F_1 \tag{3.29}$$

Moving boundary R(t) can be mapped into fixed one by following transformation equations.

$$\sigma(r,t) = \frac{r - R^*}{R(t) - R^*} \qquad \text{and} \qquad \tau(t) = t$$

Now, after some simplification,

$$\frac{\partial \sigma}{\partial r} = -\frac{\sigma}{R(\tau) - R^*} u(1,\tau)$$

where, new boundary condition becomes $0 \leq \sigma \leq 1$ and

$$\frac{dR(\tau)}{dt} = u(1,\tau)$$

Now cell density in new coordinate system $(\sigma, \tau)$ is given by

$$\tilde{x}(\sigma,\tau) = x(r,t)$$

$$\frac{\partial x}{\partial t} = \frac{\partial \tilde{x}(\sigma,\tau)}{\partial t} = \frac{\partial \tilde{x}}{\partial \tau} - \frac{\sigma}{(R(\tau) - R^*)} u(1,\tau) \frac{\partial \tilde{x}}{\partial \sigma}$$

Using Eq. (3.20)

$$\frac{\partial x}{\partial t} = F_1 - u(\sigma,\tau) \frac{\partial \tilde{x}}{\partial \tau} \frac{1}{R(\tau) - R^*} \tag{3.30}$$

Finally,

$$\frac{\partial \tilde{x}}{\partial \tau} + \left( \frac{u(\sigma,\tau) - \sigma u(1,\tau)}{R(\tau) - R^*} \right) \frac{\partial \tilde{x}}{\partial \tau} = F_1 \tag{3.31}$$

For any quantity Y, the following mathematical relation holds

$$\frac{\partial Y}{\partial r} = \frac{\partial Y}{\partial \sigma} \frac{\partial \sigma}{\partial r} = \frac{1}{R(\tau) - R^*} \frac{\partial Y}{\partial \sigma}$$

Using above identity for the velocity equation

$$\frac{1}{(\sigma(R(\tau) - R^*) + R^*)^2} \frac{1}{(R(\tau) - R^*)} \frac{\partial}{\partial \sigma} \left( (\sigma(R(\tau) - R^*) + R^*)^2 u \right) = F \tag{3.32}$$

Now for the tumor radius

$$\frac{dR(\tau)}{d\tau} = (R(\tau) - R^*)\, u(1,\tau) \tag{3.33}$$

$\sigma$ and $\tau$ can be replaced again by r and t respectively for convenience. Final equations before numerical solution are thus:

$$\frac{\partial x(r,t)}{\partial t} + A(r,t) \frac{\partial x(r,t)}{\partial r} = F_1(r,t) \tag{3.34}$$

where,

$$A(r,t) = \frac{u(r,t) - r u(1,t)}{R(t) - R^*}$$

The boundary conditions for A(r,t) are:

$$A(0,t) = 0 \qquad \text{at} \qquad r = 0 \tag{3.35}$$

and

$$A(1,t) = 0 \qquad \text{at} \qquad r = 1 \tag{3.36}$$

$$\frac{1}{(r(R(t)-R^*)+R^*)^2}\frac{1}{(R(t)-R^*)}\frac{\partial}{\partial r}\left((r(R(t)-R^*)+R^*)^2 u\right) = F \tag{3.37}$$

$$\frac{dR(t)}{dt} = (R(t)-R^*)\,u(1,t) \tag{3.38}$$

with $F_1(r,t)$ and F(r,t) defined in Eq. (3.20) and Eq. (3.26) respectively.

### 3.2.2 Numerical Solution

Two independent variables r and t are discretized by the following schemes:

r(1), r(2),...,r(J+1) for i=1,2,3,...,J+1

with, r(i+1)=r(i)+dr, r(1)=0 and r(J+1)=1.

t(1), t(2), ...,t(M+1) for n=1, 2, ...,M+1

with, t(n+1)=t(n)+dt, t(1)=0 and M=10000

Now, Eq. (3.34) is solved by FTCS scheme:

$$x(i,n) = x(i,n-1) + dt\left[F_1(i,n-1) - A(i,n-1) \times \left(\frac{x(i+1,n-1)-x(i-1,n-1)}{2dr}\right)\right] \tag{3.39}$$

Boundary conditions of A(r,t) yields following equations for x(r,t):

$$x(1,n) = x(1,n-1) + dt\,F_1(1,n-1) \qquad \forall n \geq 2 \tag{3.40}$$

$$x(J+1,n) = x(J+1,n-1) + dt\,F_1(J+1,n-1) \qquad \forall n \geq 2 \tag{3.41}$$

Initial condition is defined as:

$$x(i,1) = 0.8 \qquad \forall i \geq 1 \tag{3.42}$$

Eq. (3.37) is solved by forward difference in radial distance.

$$u(i,n) = \frac{(r(i-1)(R(n)-R^*)+R^*)^2}{(r(i)(R(n)-R^*)+R^*)^2} \times \\ (u(i-1,n) + (R(n)-R^*)\, dr\, F(i-1,n)) \tag{3.43}$$

Boundary conditions for u:

$$u(1,n) = 0 \qquad \forall\, n \tag{3.44}$$

Eq. (3.38) is solved by forward difference in time.

$$R(n) = R(n-1) + dt\,((R(n-1)-R^*)u(J+1,n-1)) \tag{3.45}$$

Matlab script for the numerical solution of reaction convection model given above is given in Appendix A.

## 3.3 REACTION-DIFFUSION EQUATION

### 3.3.1 Transformation and Numerical Solution

Eq. (2.8) in spherical coordinate with radial symmetry can be written as

$$\frac{\partial c}{\partial t} = D\left(\frac{\partial^2 c}{\partial r^2} + \frac{2}{r}\frac{\partial c}{\partial r}\right) + (\lambda - R)c\left(1 - \frac{c}{K}\right) \tag{3.46}$$

where, D, $\lambda$, R and K are diffusion coefficient(assuming homogeneous), net proliferation rate, radiation killing rate (Eq. (2.9)) and carrying capacity respectively. Initial tumor cell density value is given by Gaussian profile [21].

$$c(r,0) = \frac{1}{\sqrt{2\pi}\epsilon} e^{-\frac{1}{2}\left(\frac{r-r_0}{\epsilon}^2\right)} \tag{3.47}$$

where, $r_0$ and $\epsilon$ are the mean and standard deviation respectively. Neumann boundary condition (no flux boundary) is used as cells do not escape brain boundary (metastatic spreed of brain tumor cells outside the brain domain has not been observed so far).

$$\frac{\partial c}{\partial r} = 0 \qquad \text{for} \qquad r = 0 \qquad \text{and} \qquad r = r_{max} = 50\, mm \,(\text{for this simulation}) \tag{3.48}$$

Variables r and t are discretized as

r(1), r(2),...,r(J+1) for i=1,2,3,...,J+1

with, r(i+1)=r(i)+dr, r(1)=0 and r(J+1)=50

t(1), t(2), ...,t(M+1) for n=1, 2, ...,M+1

with, t(n+1)=t(n)+dt, t(1)=0 and M=10000

FTCS scheme is used to solve Eq. (3.46) numerically:

$$\frac{\partial c}{\partial t} = \frac{c(i,n) - c(i,n-1)}{dt} \tag{3.49}$$

$$\frac{\partial^2 c}{\partial t^2} = \frac{c(i+1,n-1) - 2c(i,n-1) + c(i+1,n-1)}{dr^2} \tag{3.50}$$

$$\frac{\partial c}{\partial r} = \frac{c(i+1,n-1) - c(i+1,n-1)}{2dr} \tag{3.51}$$

With the substitution of Eqs. (3.49) , (3.50) , (3.51) in Eq. (3.46) and after rearrangement:

$$\begin{aligned} c(i,n) =& (1-2B)c(i,n-1) + \left(B + \frac{C}{r(i)}\right) c(i+1,n-1) \\ &+ \left(B - \frac{C}{r(i)}\right) c(i-1,n-1) + dtc(i,n-1)\left(1 - \frac{c(i,n-1)}{K}\right) \end{aligned} \tag{3.52}$$

with,

$$B = \frac{Ddt}{dr^2} \qquad \text{and} \qquad C = \frac{Ddt}{dr} \tag{3.53}$$

At r=0 the term $\frac{2}{r}\frac{\partial c}{\partial r}$ diverges.

Using L' Hospital rule at r=0,

$$\frac{\frac{\partial}{\partial r}\left(\frac{\partial c}{\partial r}\right)}{\frac{\partial}{\partial r} r} = 2\frac{\partial^2 c}{\partial r^2}$$

At r =0, Eq. (3.46) can be restated as

$$\frac{\partial c}{\partial t} = 3D\left(\frac{\partial^2 c}{\partial r^2}\right) + (\lambda - R)c\left(1 - \frac{c}{K}\right) \tag{3.54}$$

In the discretization scheme:

$$\begin{aligned} c(1,n) =& c(1,n-1) + 3B\left(c(2,n-1) - c(1,n-1) + c(0,n-1)\right) \\ &+ (\lambda - A\rho(n-1)c(1,n-1)\left(1 - \frac{c(1,n-1)}{K}\right) \end{aligned} \tag{3.55}$$

Now discretization scheme for Neumann boundary condition i.e. Eq. (3.48) at r=0 is given by

$$\frac{c(2,n-1) - c(0,n-1)}{dr} = 0 \Rightarrow c(2,n-1) = c(0,n-1)$$

Finally,

$$\begin{aligned} c(1,n) =& c(1,n-1) + 6B\left(c(2,n-1) - c(1,n-1)\right) \\ &+ (\lambda - A\rho(n-1)c(1,n-1)\left(1 - \frac{c(1,n-1)}{K}\right) \end{aligned} \tag{3.56}$$

Similarly, Eq. (3.48) gives following relation at r=50 mm.

$$c(J+2,n-1) = c(J,n-1)$$

$$\begin{aligned} c(J+1,n) =& (1-2B)c(J+1,n-1) + 2Bc(J,n-1) \\ &+ (\lambda - A\rho(n-1)c(J+1,n-1)\left(1 - \frac{c(J+1,n-1)}{K}\right) \end{aligned} \tag{3.57}$$

Matlab script for the above numerical solution of reaction-diffusion model is given in Appendix B.

## 3.4 TUMOR ANTI-ANGIOGENIC DRUGS INTERACTION

### 3.4.1 Model Parameters and Numerical Solution

Rewriting Eq. (2.4), Eq. (2.5) and Eq. (2.6) of tumor anti-angiogenic drugs interaction [9] from section 2.1.

$$\frac{dV(t)}{dt} = -\lambda V \log \frac{V(t)}{K(t)} \tag{3.58}$$

**Table 3.2**: Angiostatin dosing scheme

| Dose(mg/Kg) | 4 | 4 | 4 | 4 | 4 |
|---|---|---|---|---|---|
| Days | 1 | 4 | 7 | 10 | 13 |

And,

$$\frac{dK(t)}{dt} = bV(t) - dK(t)V(t)^{\frac{2}{3}} - eK(t)g(t) \tag{3.59}$$

$$g(t) = \int_0^t c(t')e^{-\mathrm{clr}(t-t')}dt' \tag{3.60}$$

where, Eq. (3.58) and Eq. (3.59) define temporal evolution of tumor volume and carrying capacity respectively. They are solved numerically in Matlab by Euler's forward difference scheme. The constant parameters and initial values are adapted from [9]. Independent variable time is discretized as:

t(1), t(2), ...,t(M+1) for i=1, 2, ...,M+1

with t(i+1)=t(i)+dt

and t(1)=0

M=10000

$$V(i+1) = V(i) - \lambda dtV(i)\log\frac{(V(i)}{K(i)} \tag{3.61}$$

Carrying capacity with the administered anti-angiogenic drug, angiostatin [9]

$$K(i+1) = K(i) + bdtV(i) - ddtK(i)(V(i)^{\frac{2}{3}}) - edtK(i)g(i) \tag{3.62}$$

And without anti-angiogenic therapy,

$$K(i+1) = K(i) + bdtV(i) - ddtK(i)(V(i)^{\frac{2}{3}}) \tag{3.63}$$

Table 3.2 shows angiostatin dosing scheme. Treatment starts from the day one then it follows discrete scheme i.e boli. A constant gap of 3 days is maintained after

day seven.

Matlab script of Hahnfeldt's model is given in Appendix C.

# CHAPTER 4
# RESULTS AND DISCUSSION

## 4.1 RESULTS

First part of this research work aims to validate survival time which is the time difference of the first diagnosis and the time for the radius of tumor to reaches 40 mm, given in reaction-convection model [13], [26]. The survival time is different based on the extent of resection (total or partial) of tumor, radiation treatment modality, and chemotherapy dosing scheme. Radiation treatment is also variant upon following factors:

1. Total dose,number of fractions and dose per fraction (Standard scheme: 2 Gy daily dose with the 30 fractions in total of 60 Gy)

2. Treatment starting time after surgery (usually starts from 6 weeks and radiation is then given for next 6 weeks)

As described in Section 2.2.3, total resection corresponds to removal of tumor sphere of radius 20 mm while radius of partial resection is taken to be equal to 18 mm in [13]. Major finding based on the statistical analysis of GBM patients in [13], [29], and [26] are:

1. Life expectancy for the time when GBM is diagnosed is typically one year

2. Patients who underwent partial resection had 6.6 times higher risk of death compared to those who went complete resection [26].

3. Patients treated by radiation(after resection) had 0.26 times lower risk of death without it (for the resection of GTV>98%).

4. MST was 14.6 months for patients who underwent radiotherapy plus chemotherapy

(Temozolomide) compared to 12.1 months for radiotherapy alone.

Specifically, the result of this work is compared with the outcome of [13] and [29] that was based on a statistical analysis of a group of patients between the age of 20 and 39 (Table 4.1).

Units for the time and length scale for reaction-convection model are given in weeks and millimeters respectively.

Radiotherapy treatment is based on the scheme highlighted in Section 2.2.1 [13] which essentially uses linear quadratic model (Eq. (2.9)) with some fixed value of radio sensitivity parameter $\alpha$ and fractionated radiation. This research work is also intended to observe the variation (if any) of survival time (MST) of glioblastoma patients by changing the value of $\alpha$ and, by using different fractionation scheme.

The following radiation modalities are being tested in clinical practice to see better outcome (if any) in survival time of glioblastoma patients:

1. Hyperfractionated: Hyperfractionated means giving more than one treatment of radiotherapy per day. Continuous hyperfractionated radiotherapy gives treatment 3 times a day for 12 days (excluding the weekend). By doing this, radiation treatment can be completed within two weeks from the starting week ($6^{th}$ week after diagnosis) but the number of fraction remains the same along with dose per fraction and, hence, total dose.

2. Hypofractionated: It refers to the large dose given in the less number of treatment fractions which means, for example, giving 6 Gy dose and reducing number of fractions to 15 without altering entire treatment duration along with fixed total dose.

The above radiation schemes can be implemented in the mathematical models given by [11] and [13] by altering the values of number of fractions and dose per fraction, keeping, the same total dose to draw conclusion about their effectiveness (if any).

Table 4.1 lists the median survival time given in [13]. Complete refers to complete re-

**Table 4.1**: Median survival time (MST) for different treatment modalities

| Treatment | Complete, RT | Partial, RT | Partial only | Partial, RT, and Chemo |
|---|---|---|---|---|
| MST | 92 (Weeks) | 46 (Weeks) | 15 (Weeks) | 60 (Weeks) |

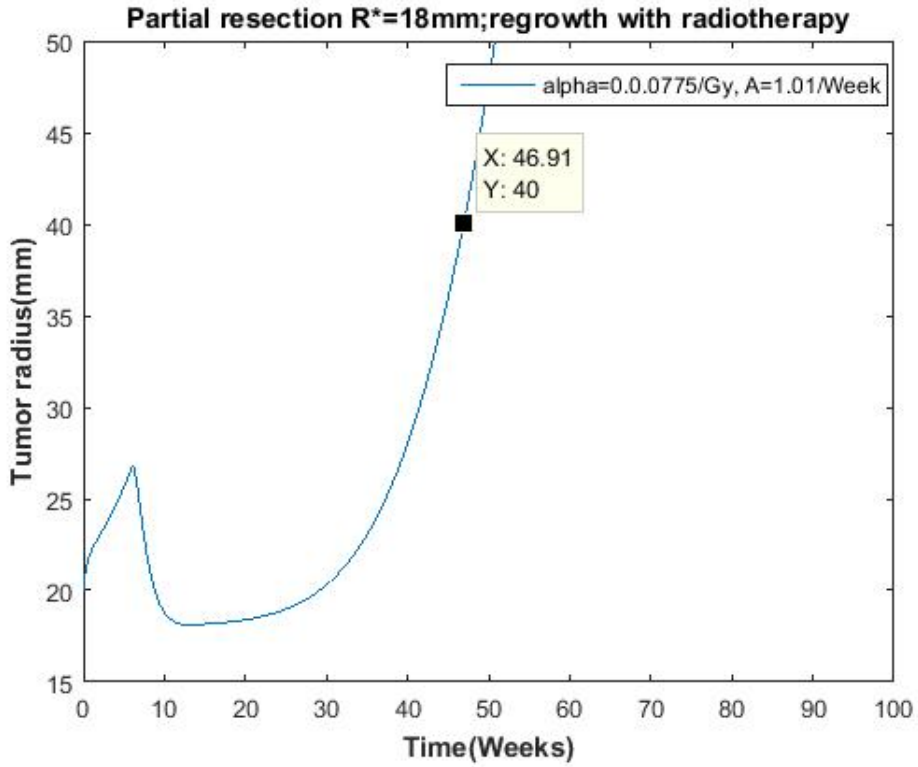


**Figure 4.1**: Partial resection (18mm) and Radiotherapy

section ($\approx$ 20 mm) while partial refers to partial resection of the tumor radius of value equal to 18 mm. The terms RT and Chemo refer to radiotherapy and chemotherapy respectively.

Figure 4.1 shows the growth of tumor after partial resection ($R^*$=18 mm) with radiotherapy. Radiation killing rate A is taken to be equal to 1.01/week and which is equivalent to radio sensitivity parameter, $\alpha$ close to 0.0775/Gy with standard radiotherapy fractionation scheme (30 fractions with 2 Gy daily in the total of 60 Gy) and

$\frac{\alpha}{\beta}$ ratio equal to 10 Gy (for actively proliferating cells). Survival time (corresponding to R=40 mm) is approximately 46 weeks. Regrowth of tumor after resection occurs aggressively before intervention by radiotherapy which starts from 6 weeks. After relatively stable period, it starts regrowing quickly.

Survival time becomes longer when the same treatment modality with the same parameter values, is offered except radiotherapy killing rate A which is now 1.687/week (equivalent to radio sensitivity parameter $\alpha$ equal to 0.137/Gy). Survival time in this scheme becomes 69 weeks approximately as shown in figure 4.2

Figure 4.3 shows the growth of tumor radius using radiotherapy under hyperfractionated scheme. It implements radiation delivery of 2 Gy given thrice a day (excluding weekends) without altering number of fractions and total dose. Treatments last for two weeks (from $6^{\text{th}}$ to $8^{\text{th}}$) only. Survival time is found to be lower than the standard treatment option.

However, survival time increases significantly under the treatment using hypofractionated scheme (Figure 4.4) then hyperfractionated scheme (around 76 weeks compared to 25 weeks). Under this scheme, a dose of 4 Gy per fraction is given. This results a reduction in the number of fraction from 30 to 15 without changing standard, total dose which is 60 Gy. Treatment duration remains same as standard scheme i.e. from $6^{\text{th}}$ to $12^{\text{th}}$ weeks.

Figure 4.5 shows the growth of tumor radius after partial resection ($R^*$=18 mm) with radiotherapy and chemotherapy. Survival time is close to 57 weeks. Chemotherapy dosing follows the scheme described in Eq. (3.18) with the radiation scheme same as Figure 4.1.

Figure 4.6 shows the growth of R(t) after the complete resection ($\approx$20 mm) and radiotherapy. Radiotherapy scheme is same as before (Figure 4.1). Survival time is close to 92 weeks indicating the importance of total resection for significant improvement.

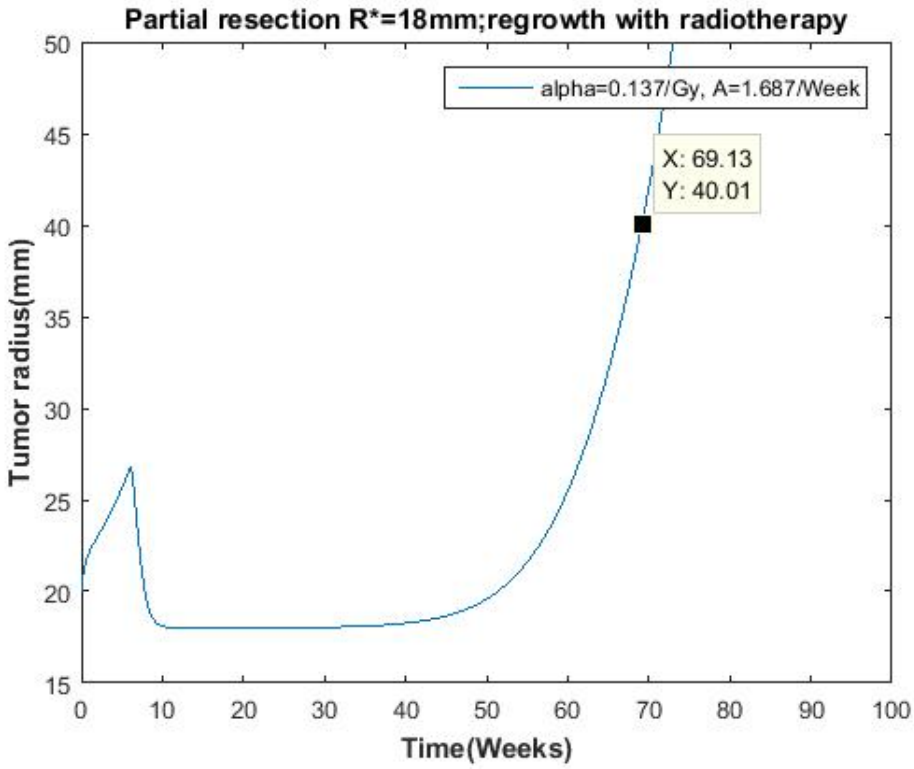


**Figure 4.2**: Partial resection (18mm) and Radiotherapy

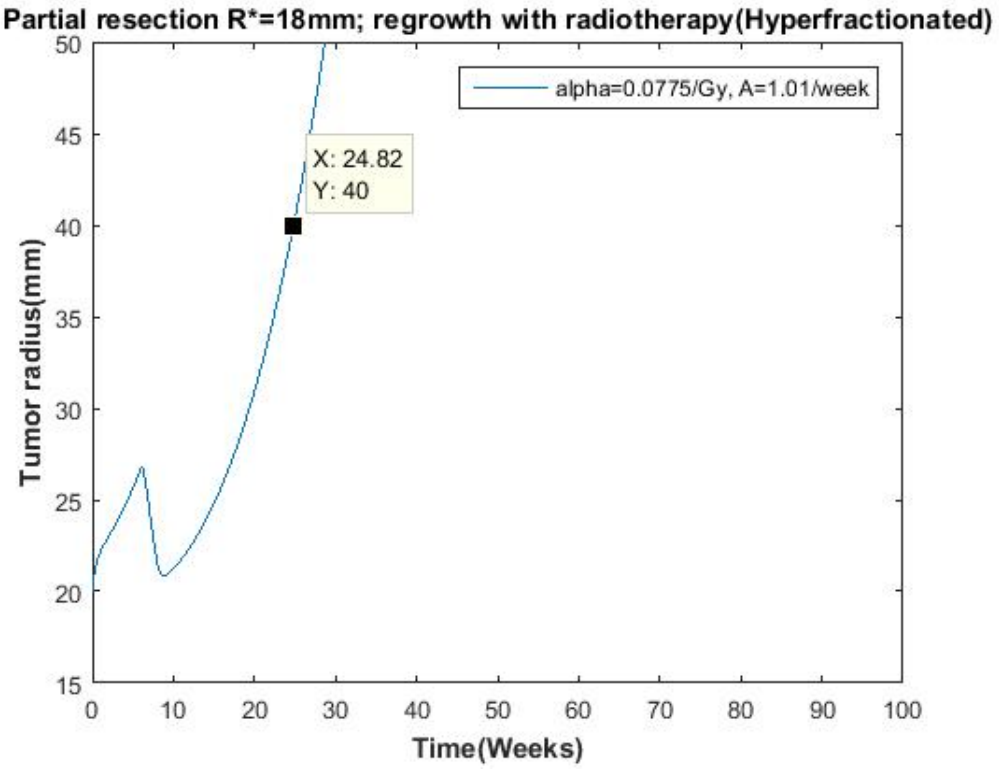


**Figure 4.3**: Hyperfractionated radiation treatment scheme

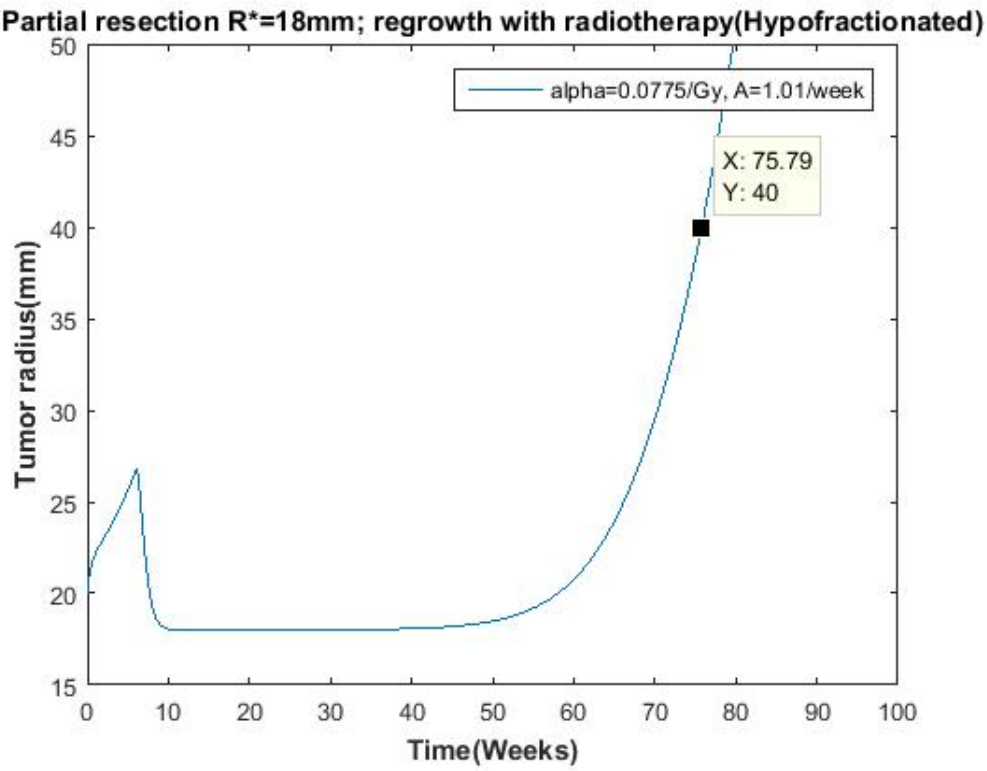


**Figure 4.4**: Hypofractionated radiation treatment scheme

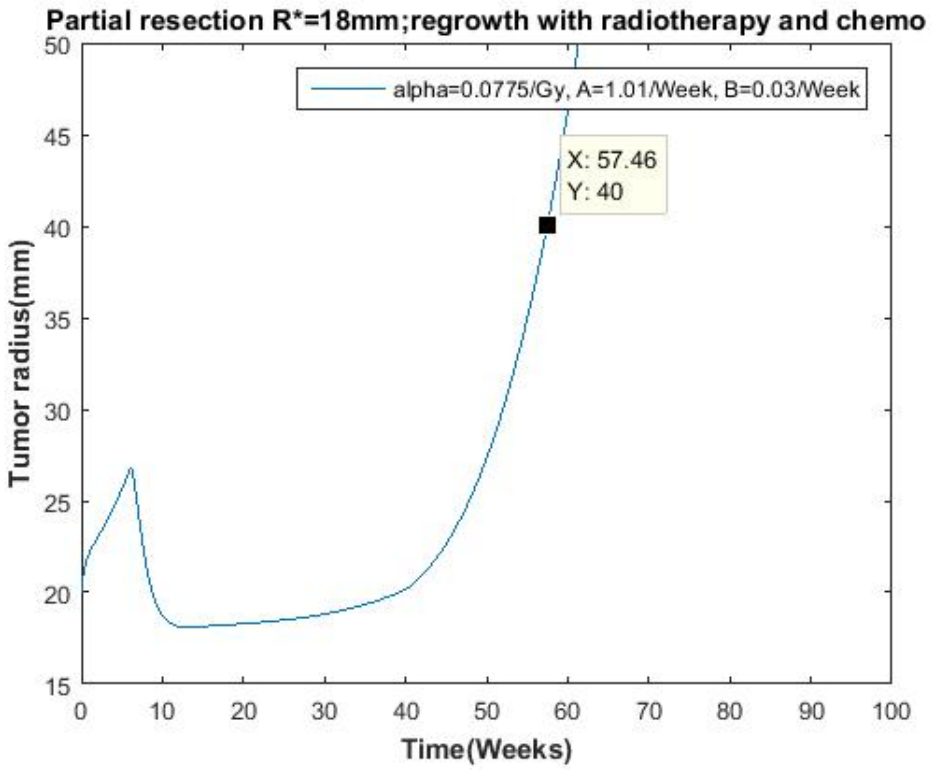


**Figure 4.5**: Partial resection (18 mm), Radiotherapy, and Chemotherapy

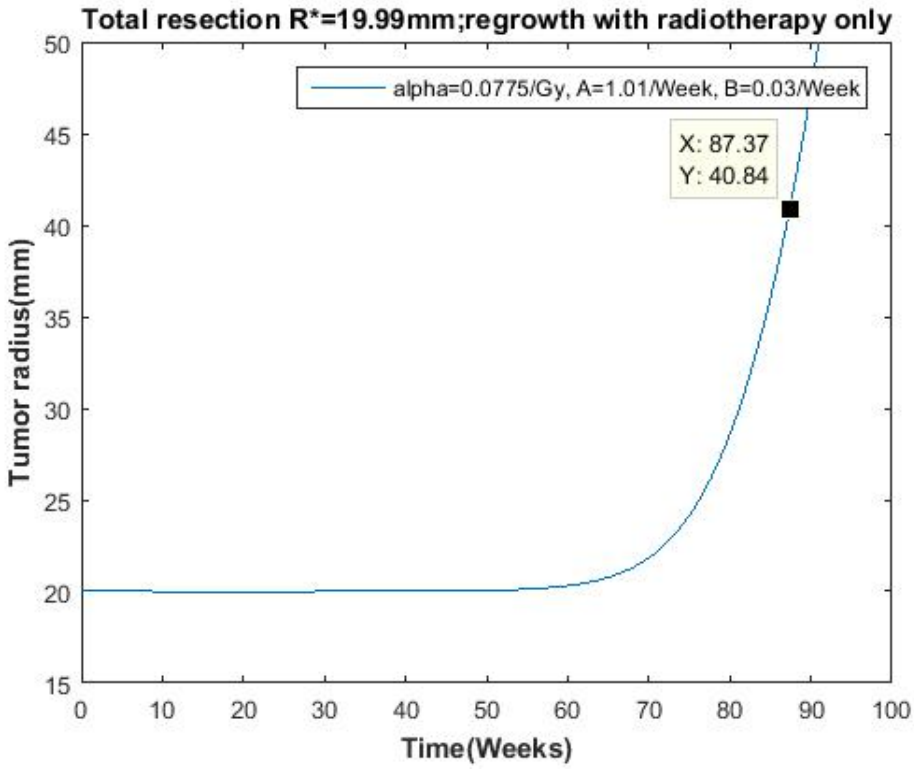


**Figure 4.6**: Total resection (19.99 mm) and Radiotherapy

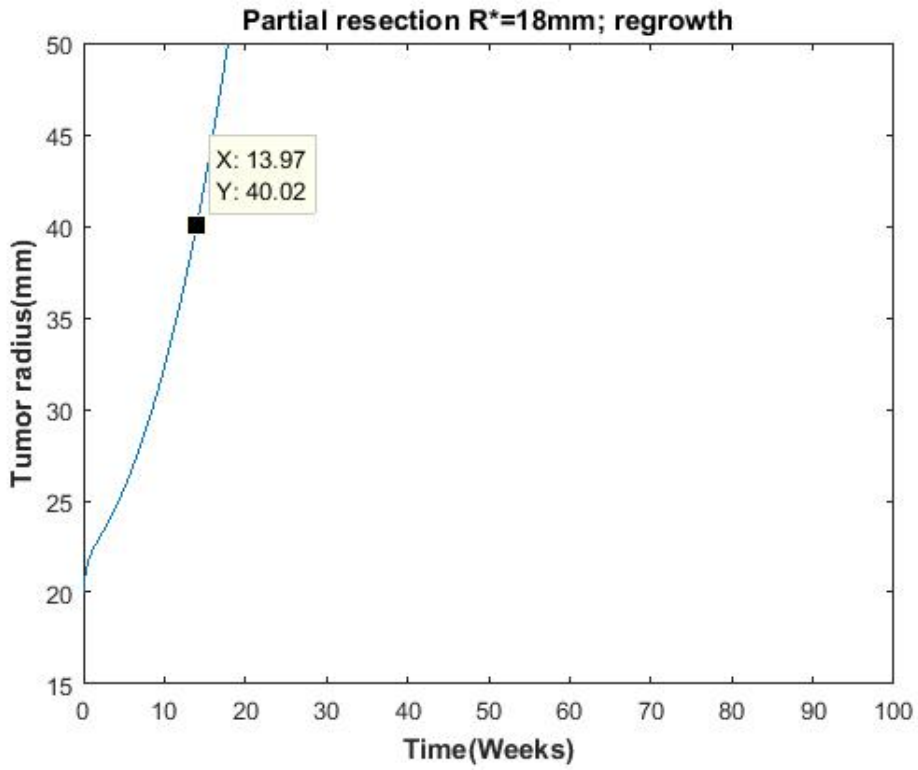


**Figure 4.7**: Partial resection (18 mm) only

Figure 4.7 represents growth pattern of radius R(t) without using radiotherapy and chemotherapy. Survival time is close to 14 weeks which essentially indicates the requirement of radiotherapy and chemotherapy for the longer survival benefit.

In the second part, this research work aims to draw conclusion from the numerical solution of reaction-diffusion equation Eq.(2.8) proposed by [11]. For the numerical solution, brain domain of range 5 cm (50 mm) has been assumed. The initial Gaussian tumor density profile has been assumed to be originating from 2.5 cm. The entire calculation has been performed in spherical coordinates with radial symmetry, which, resembles the tumor spheroid.

Fundamental components of the equation are net proliferation rate $\rho$ and diffusion coefficient (D). The net proliferation term accounts for the uncontrolled growth (mitotic) of tumor cells while diffusion coefficient characterize the passive diffusion by

which tumor cells invade nearby healthy cells. As mentioned in Section 2.2.2, these two events are mutually exclusive (Go or grow hypothesis). Invisibility index which is the ratio of diffusion coefficient and the net proliferation rate i.e. ($D/\rho$), determine overall nature of tumor whether it is diffusion dominated (vascular) or proliferation rate dominated (avascular). Also, selection of higher value of diffusion coefficient means invasion is preferentially along the white matter tract which is similar to the trend by which flow of water exhibits anisotropic diffusion along the white matter.

Two conclusions can be drawn from the value of invisibility index immediately:

1. $\frac{D}{\rho} > 1$ for diffusion dominated growth of tumor cell density
2. $\frac{D}{\rho} < 1$ for isolated growth of tumor cell density

Patient specific parameters, diffusion coefficient (D), net proliferation rate ($\rho$), and radio sensitivity parameter ($\alpha$) are chosen from Table. 2 (Patients 2 and 5) of [14]. Length and the time units for all calculated parameters and constant parameters are expressed in millimeter and day respectively.

Figure 4.8 and Figure 4.9 compare the tumor density profile versus radial distance at the same time with two different invisibility indices. Tumor density value at t=20 days is 50 corresponding to invisibility index 0.594 while it is approximately equal to 15 for invisibility index value of 1.59. Less diffusion indicates higher accumulation of tumor cells and vice-versa. This also indicates that the proliferation and diffusion do not occur side by side.

Figures 4.11 and 4.10 are the corresponding tumor density plots for two values of invisibility index.

Figures 4.12 and 4.13 are the number density plot against radial distance at three different times (with the same value of invisibility index) for the reaction-diffusion model with radiotherapy killing term defined in Eq. (2.10). Approximate number density values are 22 and 12 corresponding to the values of $\alpha$, 0.137/Gy and 0.0775/Gy respectively. Under the fractionated radiotherapy with the fixed number of fractions,

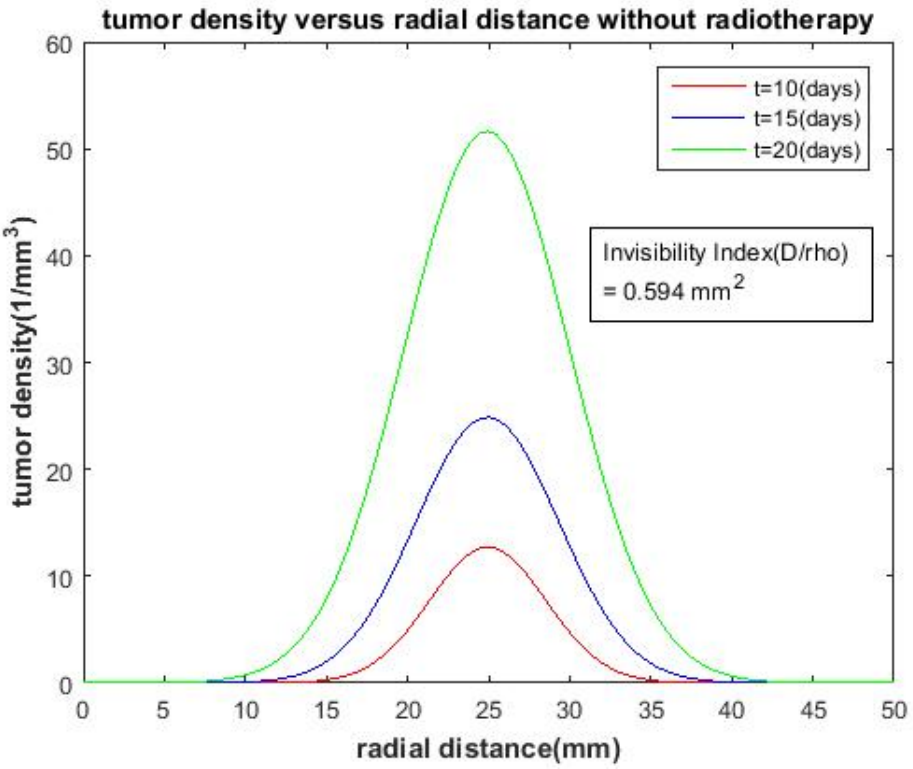


**Figure 4.8**: Tumor density versus radial distance at different time with lower invisibility index (0.594 $mm^2$)

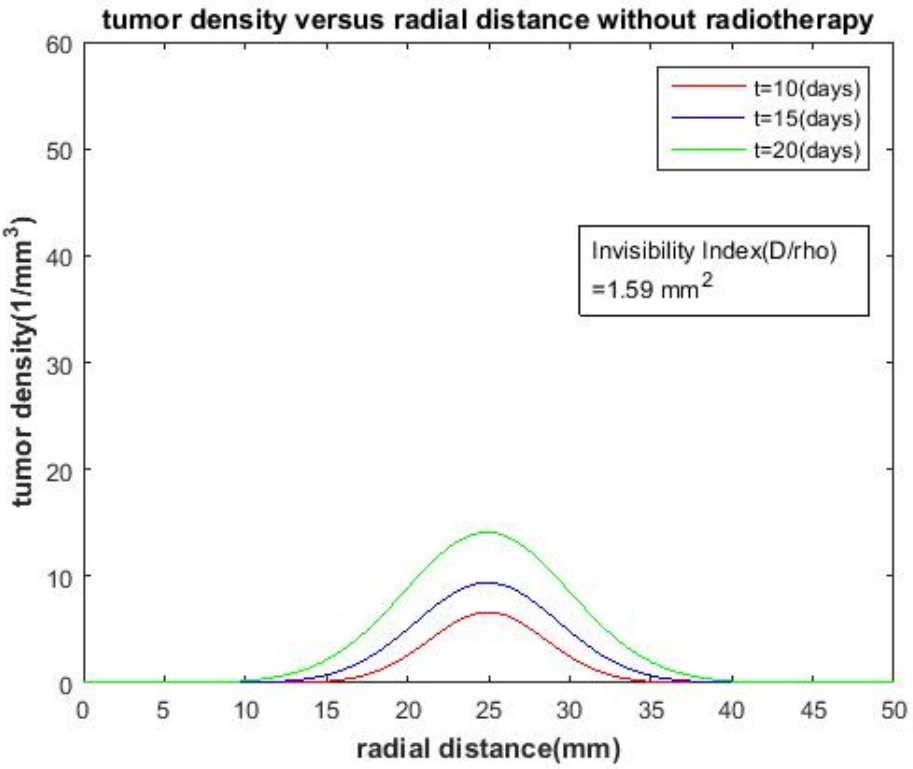


**Figure 4.9**: Tumor density versus radial distance at different time with higher invisibility index (1.59 $mm^2$)

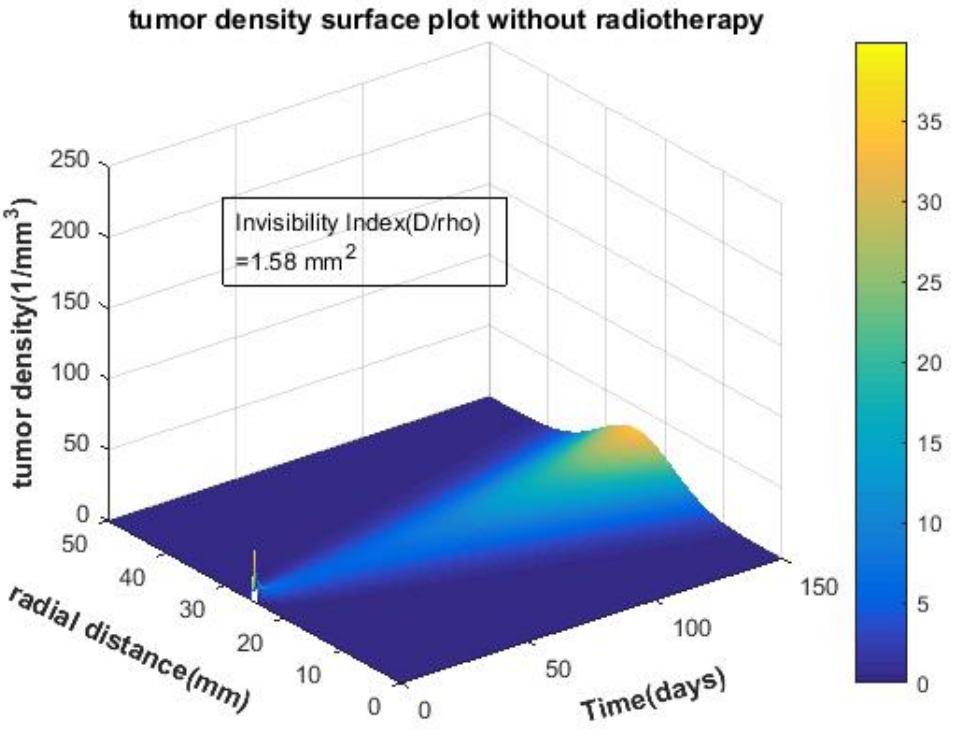


**Figure 4.10**: Tumor density surface plot at higher invisibility index (D/rho=1.59 $mm^2$) without using radiotherapy

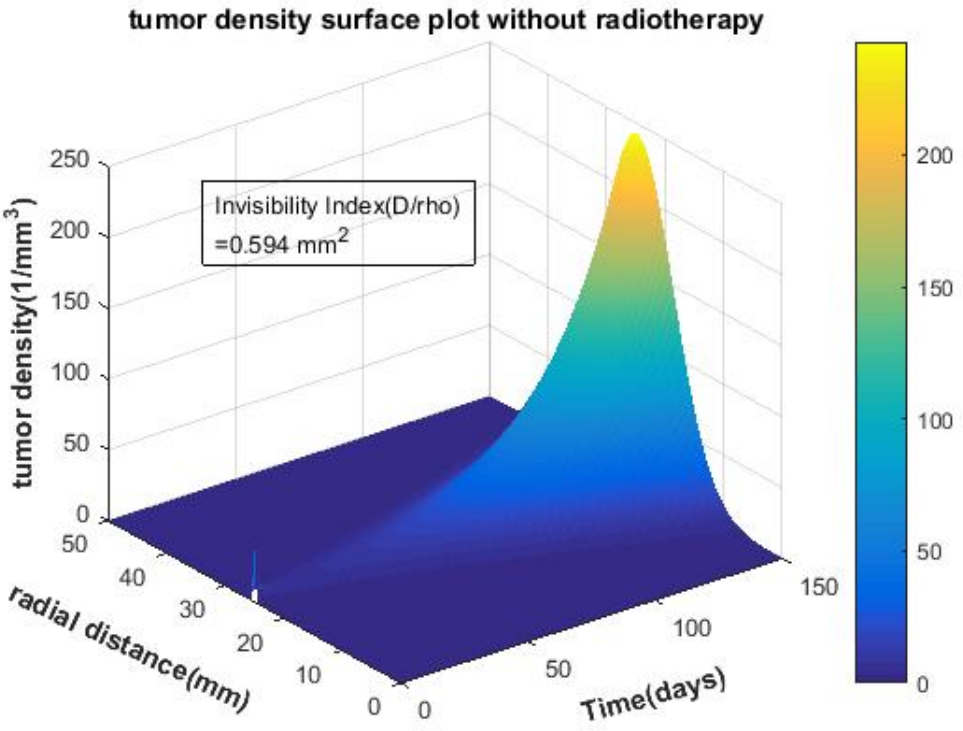


**Figure 4.11**: Tumor density surface plot at lower invisibility index (D/rho=0.594 $mm^2$) without using radiotherapy

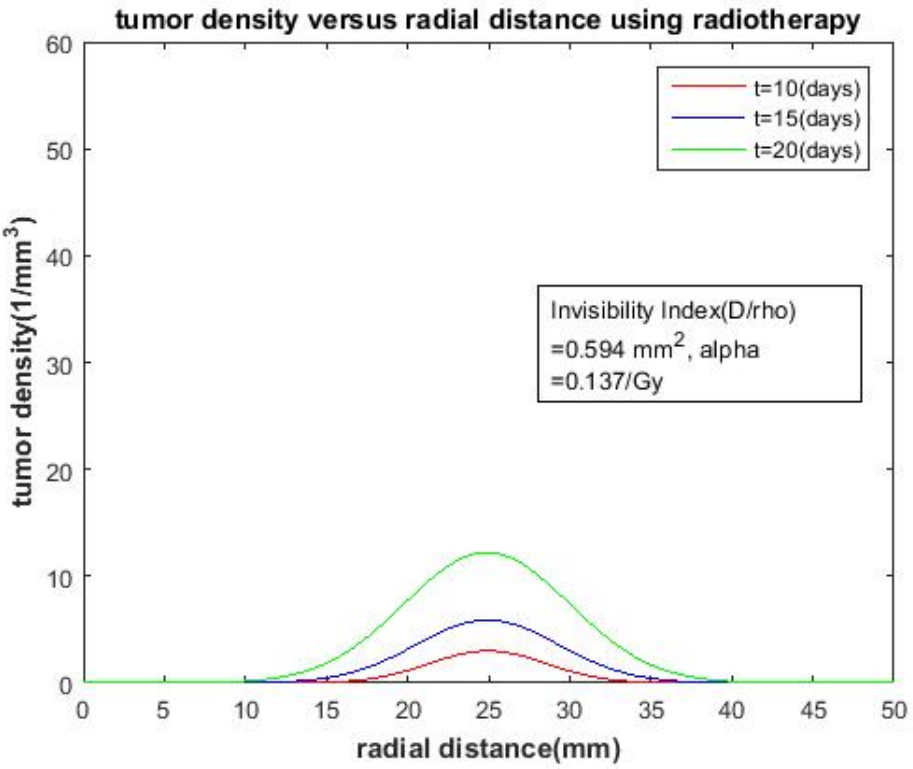


**Figure 4.12**: Tumor density versus radial distance at different times with higher radio sensitivity parameter, $\alpha$=0.137/Gy

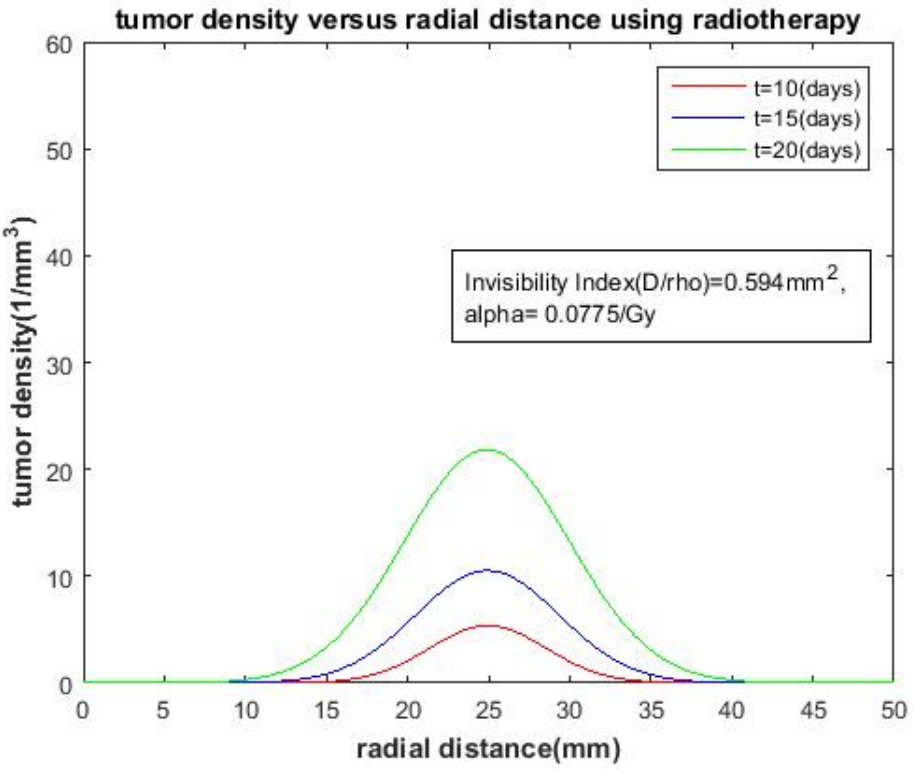


**Figure 4.13**: Tumor density versus radial distance at different times with lower radio sensitivity parameter, $\alpha$=0.0775/Gy

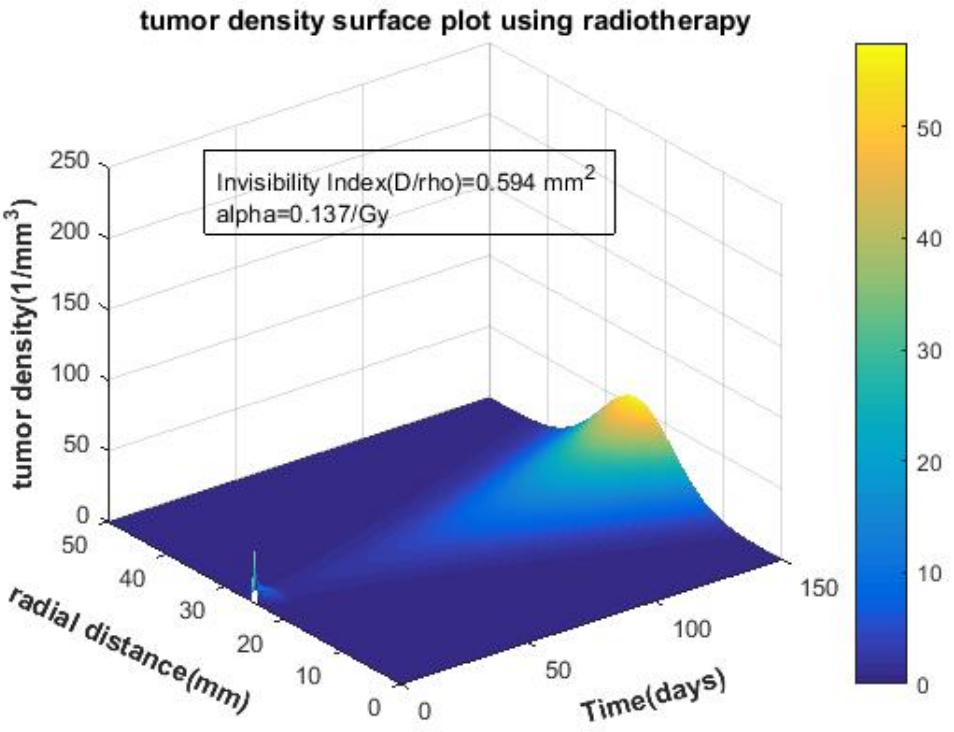


**Figure 4.14**: Tumor density surface plot at higher radio sensitivity parameter, $\alpha$=0.137/Gy

dose per fraction and total dose; choice of $\alpha$, radio sensitivity parameter, is only influencing factors that can alter the value of killing rate and hence, tumor cell density. Higher sensitivity of cells toward the radiation means higher value of $\alpha$, which causes more tumor cells damage. This ultimately causes number of cells left in a volume of interest i.e. cell density dropping down. Figures 4.14 and 4.15 are the surface plot of tumor cell density for the two values of $\alpha$ used in Figures 4.12 and 4.13

Figure 4.16 is the surface plot of cell density values (at fixed t=10 days) by varying radial distance and alpha-beta ratio ($\frac{\alpha}{\beta}$), also called tissue response factor.An optimum value of $\frac{\alpha}{\beta}$ =10 Gy in Figure 4.16 validates the assumption that for actively proliferating glioma cells (early responding) it is equal to 10 Gy.

Another approach for describing tumor growth is based on Hahnfeldt's [9] model (Eq. (2.4) and Eq. (2.5)) which relates rate of change tumor volume with stimulatory and

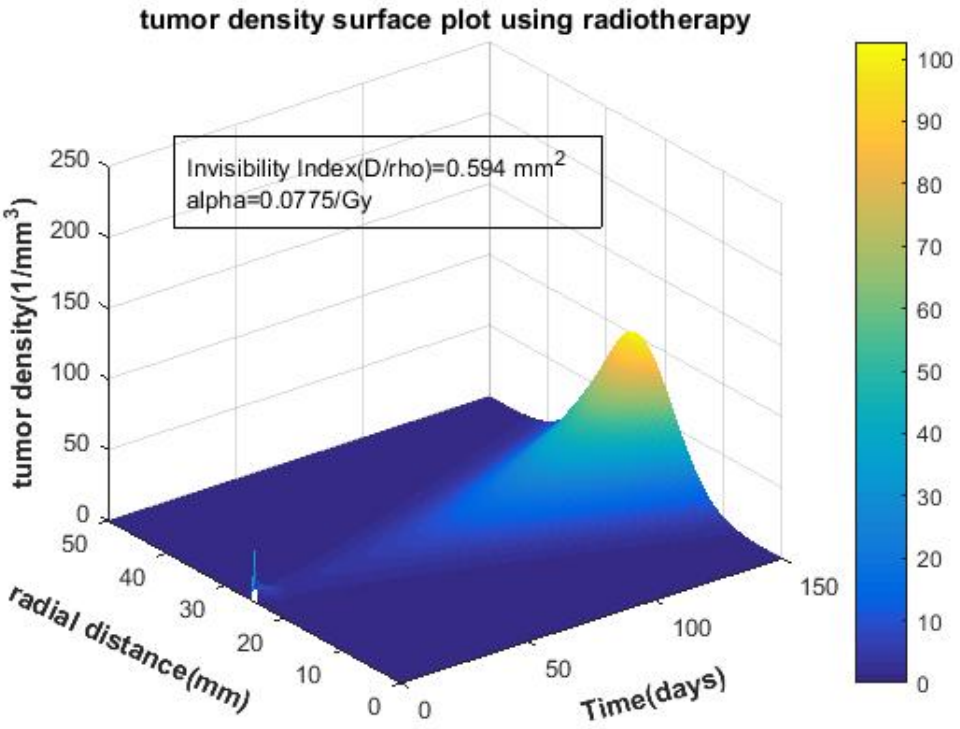


**Figure 4.15**: Tumor density surface plot at lower radio sensitivity parameter, $\alpha$=0.137/Gy

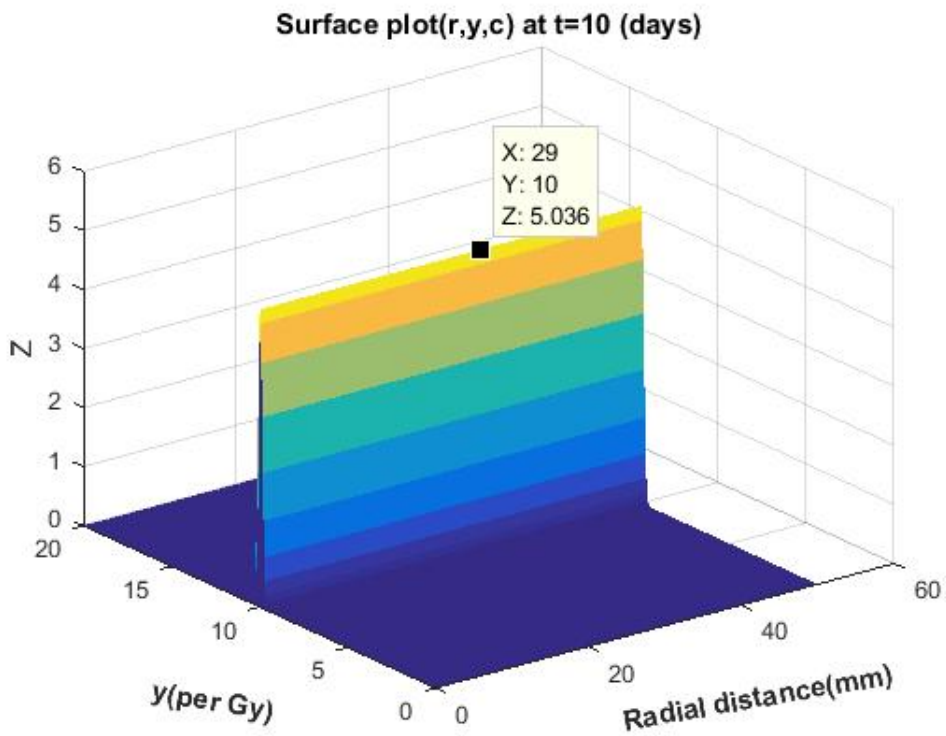


**Figure 4.16**: Variation of tumor cell density around optimum value of alpha-beta ratio (x=10 Gy) at t=10 (days)

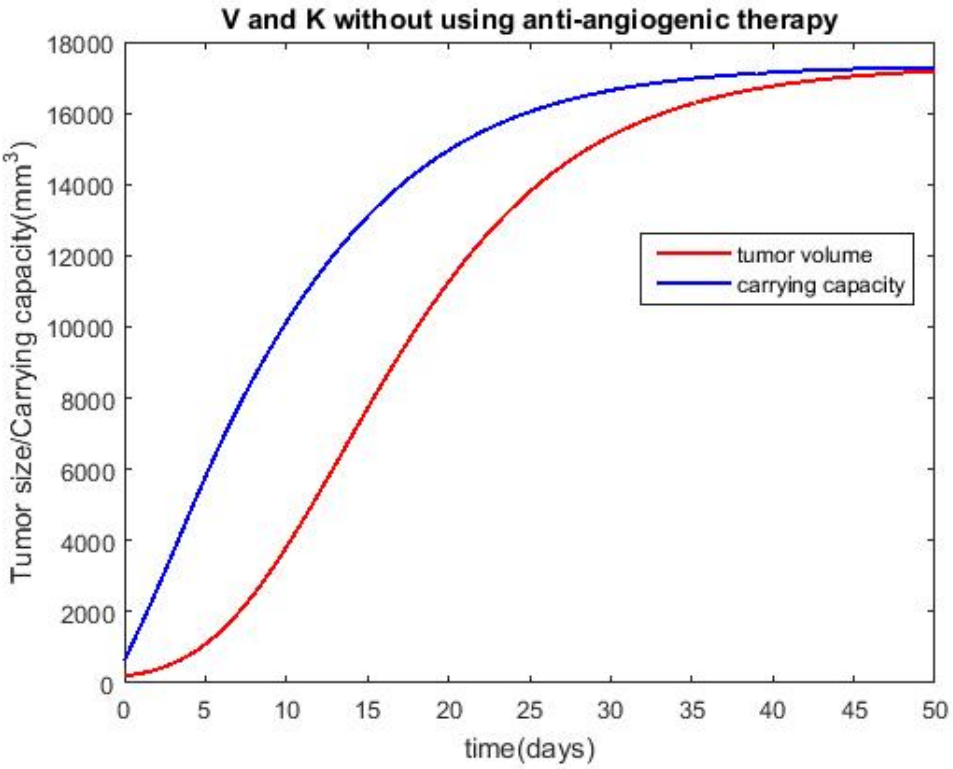


**Figure 4.17**: Tumor volume and carrying capacity versus time

inhibitory effects induced by tumor itself. Due to these effects, carrying capacity i.e. tumor bed, also changes with time. As described in section 2.1 angiogenesis is initiated by various stimulatory factors which create neovascularization and ultimately tumor volume and carrying capacity increase with time. Inhibitors (naturally occurring or artificially administered) attempt to slow down angiogenesis by blocking simulators like VEGF. Delivery of anti-angiogenic drugs like angiostatin to slow down the growth of tumor volume and carrying capacity by blocking growth of angiogenic simulators, is called anti-angiogenic therapy.

Initial values and parameters value involved in Eq. (2.4) and Eq. (2.5) are taken from [9]. Units of the dimension of length and time are expressed in millimeters and days respectively.

Figure 4.17 represents Gompertizian growth of tumor volume and carrying capacity without artificially administered anti-angiogenic drugs. Initial growth of both tumor volume and carrying capacity is nearly exponential however they saturate due to insufficient nutrients and limited space. Tumor volume reaches its upper threshold i.e. carrying capacity at sufficiently large time ($\approx$ 45 days).

Figure 4.18 represents tumor volume and carrying capacity under the anti-angiogenic drug scheme as given in Table 3.2. Drugs are given in $4^{th}$ day, $7^{th}$ day, and then every three days after. Due to this there is a sharp decrease in carrying capacity however it again increases. Approximate values for carrying capacity without and with angiogenic drugs for $10^{\text{th}}$ day is around 10,000 and 7,000 $\text{mm}^3$ respectively indicating that there is an effectiveness of anti-angiogenic drugs to some extent.

The constant parameters b and d represent rate by which simulators and inhibitors are produced by tumor. According to Hahnfeldt [9], numerical value of these parameters are b=5.85/day and d=0.0873/day , and generated from the Gompertz fit.

Figure 4.20 and 4.22 are the surface plot of carrying capacity and tumor volume by

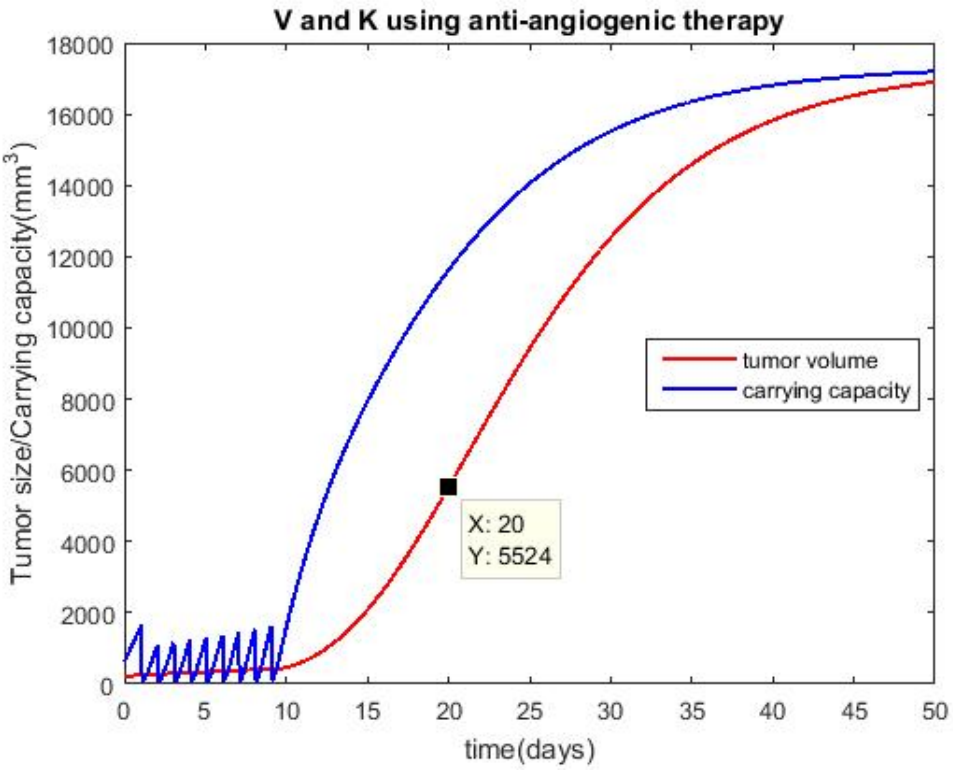


**Figure 4.18**: Tumor volume and carrying capacity versus time with administered anti-angiogenic drug

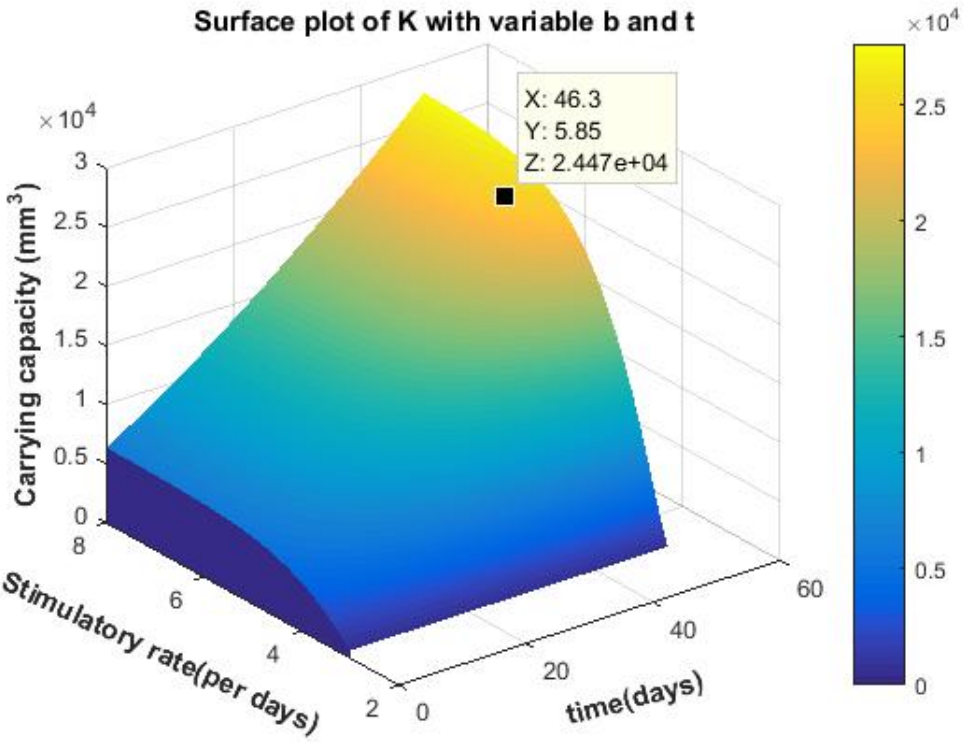


**Figure 4.19**: Carrying capacity surface plot with time and variable stimulatory rate (b)

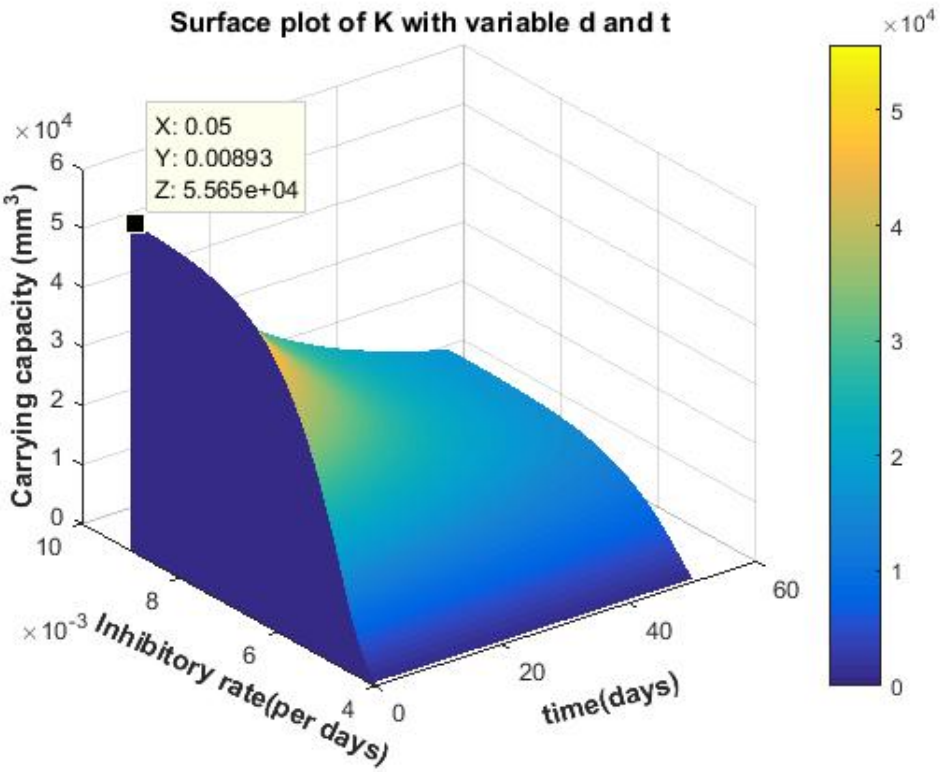


**Figure 4.20**: Carrying capacity surface plot with time and variable inhibitory rate (d)

assigning variable values of d around its optimum value, along with the variable time. Maximum values of carrying capacity and tumor volume are found to be satisfying optimal value of b i.e. 0.0873/day which is thus a reasonable choice based on the surface plot (Figures 4.20 and 4.22).

Similar are the trend for the validation of the optimum value of stimulatory rate (b=5.85/day) based on the results in Figures 4.19 and 4.21.

## 4.2 DISCUSSION

Survival time calculated using simple numerical scheme for the reaction-convection model proposed [13], are all in agreement with the values obtained using transformed and simplified ordinary differential equation [22]. There is better outcome in the sense of survival time for using standard treatment modality which consists of surgery fol-

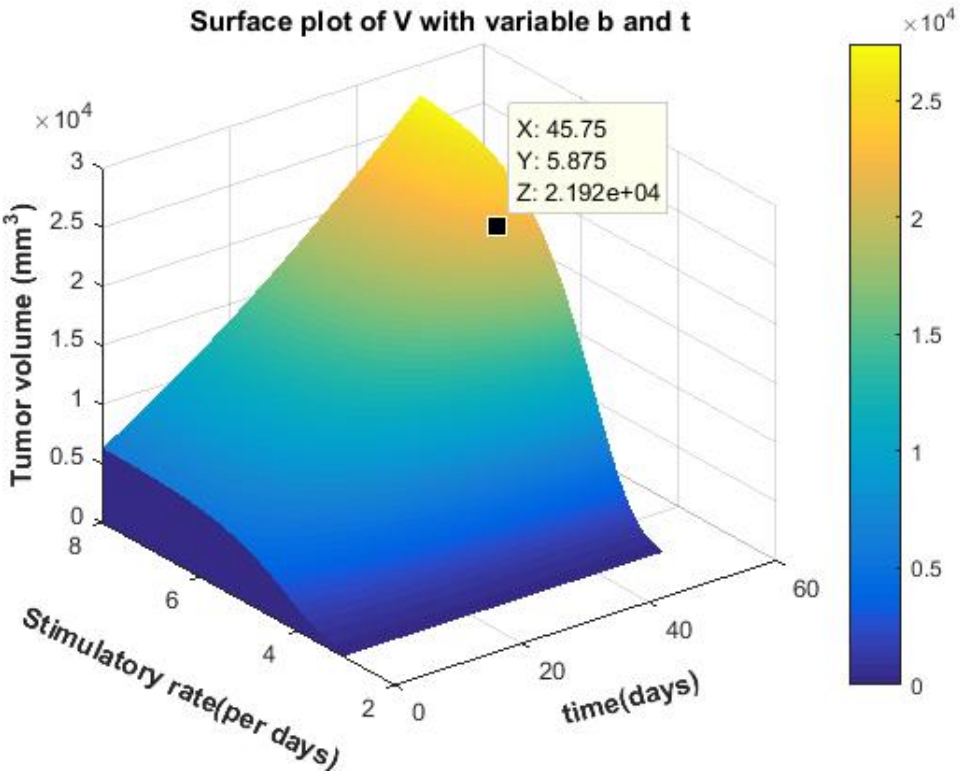


**Figure 4.21**: Tumor volume surface plot with time and variable stimulatory rate (b)

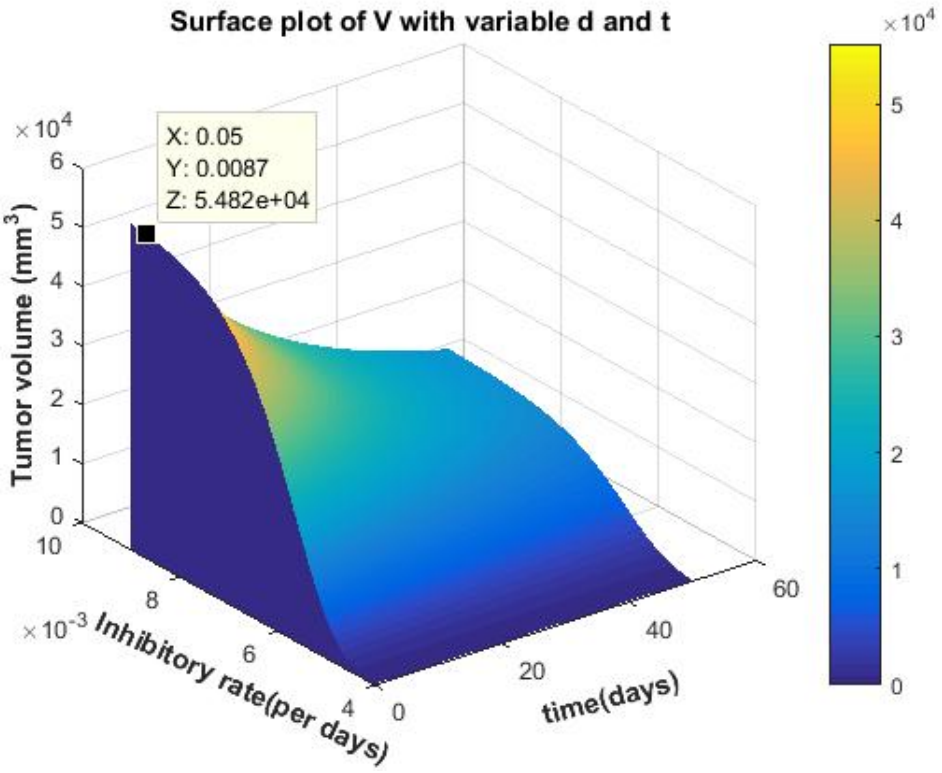


**Figure 4.22**: Tumor volume surface plot with time and variable stimulatory rate (d)

lowed by radiotherapy and chemotherapy. Survival time also increases significantly in case of total resection and adjuvant radiotherapy. Radiotherapy under hypofractionated scheme is found to be better option than hyperfractionated scheme although survival time has not been associated with the normal tissue complication such as its necrosis and cognitive failure of the brain.

Reaction-diffusion model is another approach of continuum model which accounts primarily passive diffusion, main contributing factor for the migration of tumor cells. Qualitatively, tumor density variation with various parameters like diffusion coefficient, net proliferation rate and radiotherapy parameters (of linear-quadratic model Eq. (2.10)) show predicted results. Numerical calculation of above two tumor growth modalities resembles actual tumor growth *in vivo* if patient specific parameters like proliferation rate, diffusion coefficient etc are known precisely prior to the modeling. Tumor density evolution can be monitored exactly if its initial value truly resembles with those initial value of the tumor during the time when MRI images are taken. By doing this, there will be a perfect match between initial value with the patient specific parameters like net proliferation rate. Numerical calculation chooses single value of the diffusion coefficient which is, in fact, simply not true as there is inhomogeneity in brain composition due to white matter, gray matter and CSF, distributed in a different proportion. Thus, inhomogeneity needs to be addressed in the numerical calculation. There are different active transport phenomena like chemotaxis by which tumor cells are driven along with the passive diffusion. There will be better result if diffusion term in reaction-diffusion model accounts for all possible transport (both active and passive).

Numerical solution of tumor volume and carrying capacity growth models proposed by Hahnfeldt [9] is also presented in result. Anti-angiogenic drugs have shown good impact on the slowing down of the tumor volume and carrying capacity. This model is different from previous models (reaction-convection, reaction-diffusion) in the sense

that the growth of tumor volume is considered in stead of density. However, it does not account the spatial variation. Tumor growth becomes predominantly diffusion dominated after it enters in metastatic phase which definitely necessitates the importance of spatial effect to take into the account.

# CHAPTER 5
# CONCLUSIONS

The purpose of this research is to validate various forms of mathematical modeling of glioblastoma multiforme (GBM) expressed as differential equations, numerically. The first work was involved in the numerical solution of the reaction-convection model, efficacy of which is expressed in terms of survival time. It was calculated using simple numerical scheme for the standard-of-care treatment in clinics which includes surgery followed by the radiation and chemotherapy. Survival time using all treatment options increased significantly to 57 weeks compared to that of surgery, close to 14 weeks. It was also observed that survival time increased significantly to 90 weeks if tumor is totally resected. Survival time was also found to be increasing significantly to 75 weeks in hypofractionated radiotherapy scheme compared to 24 weeks in the case of hyperfractionated radiation treatment. Survival time was also influenced by different values of radiation killing rate A, which depends primarily on radiosensitivity parameters $\alpha$ in the context of actively proliferating glioma cells. Survival time was equal to 69 weeks for radiation killing rate A equal to 1.687/week ($\alpha$=0.137/Gy) compared to 46 weeks for A equal to 1.01/week ($\alpha$=0.0775/Gy). This result however has implementation difficulty *in vivo* as glioblastoma cells are known to be highly radioresistant. In reaction-diffusion model using simple numerical scheme, tumor cell density patterns due to variation in patient specific tumor parameters such as net proliferation rate and diffusion coefficient were computed. Significant differences were observed in the patterns while using dominant diffusion and proliferation rate separately ('Go or grow hypothesis'). Qualitatively, results were similar for the tumor cell density pattern while using radiotherapy with the same values of radiation killing

rate A (defined as R in this model) and hence radiosensitivity parameter $\alpha$, used in reaction-convection model. Numerical solution of the tumor growth model under the anti-angiogenic therapy revealed some impacts in optimum tumor growth control however it was not significant. Optimum value of parameter alpha-beta ratio ($\frac{\alpha}{\beta}$) of linear quadratic model used in reaction-convection and reaction-diffusion models was tested by making tumor density surface plot of $\frac{\alpha}{\beta}$ in the vicinity of its optimum value (10 Gy for actively proliferating glioma cells) and radial distance at fixed time. The maximum concentration of density around 10 Gy validated the purpose. Similar procedures were applied for constant parameters, stimulatory rate (b) and inhibitory rate (d), in anti-angiogenic therapy [9] to validate their constant values.

# APPENDICES

# APPENDIX A

# MATLAB SCRIPT: REACTION-CONVECTION MODEL

```
% Equations related
%Number density equation
%        dx/dt+A*dx/dr=beta*x((((mu+lambda-delta)/beta)-1/beta(A1*rho(t)
%+B*tau(t)))-x):

%        dx/dt+A*dx/dr=beta*x(K-x) &F1=beta*x(K-x)& A=u-u(1,t)*r
%Radial velocity equation
%        (1/s^2)d(s^2u)/dr=beta*x-mu with F=beta*x-mu with s=r*(R(t)-R*)+R*
%Tumor growth radius
%        dR/dt=(R(t)-R*)u(1,t) (Boundary condition1)
%          u(0,t)=0
%constant parameters
clear
clc
 lambda=(2*24*7/100);  %Tumor cells Proliferation rate (in per weeks)
mu=(24*7/72);         %Necrotic cells removel rate (in per weeks)
delta=(1.89*24*7/100);%Rate of cells becoming necrotic (in per weeks)
theta=1000000; %Total density of tumor and necrotic cells(constant)
 beta=lambda+mu;%constant
 A1=1.687;          %Radiotherapy killing rate (in per weeks)
B=0.03;         % Chemotherapy killing rate (in per weeks)
alpha=0.137;%Radiosensitivity parameter of linear-quadratic(LQ)model
d=4;          %Dose per fraction (Gy)
n_frac=15;    % Number of radiation fractions

%Discretization of proliferation rate (assuming it as a variable)
r0=0;         %initial value of radial distance.
rf=1;         %final value of radial distance.
```

```
dr = 0.01;    %distance step
J=(rf-r0)/dr;
t0=0;         %initial time
dt = 0.01;    %time step.
tf=100;
M=tf/dt;
R0=20;       %Initial radius
R_a=18;      %R*: Radius of resected tumor.
% R_a=19.99; %Radius of totally resected tumor
%Initializing matrix

r=zeros(J+1,1);
t = zeros(M+1,1);
R = zeros(M+1,1);
x = zeros(J+1,M+1);
u=zeros(J+1,M+1);
A=zeros(J+1,M+1);
F1=zeros(J+1,M+1);
F=zeros(J+1,M+1);
rho=zeros(M+1,1);
tau=zeros(M+1,1);
% lambda=zeros(N+1,1);
% lambda(1)=lambda_0;
% for k=1:N-1
%     lambda(k+1)=lambda(k)+dl;
% beta(k)=lambda(k)+mu;%constant
%Initializing values
t(1) = t0;
r(1)=r0;
 R(1)=R0;
        x(1,1)=0.9;
        %scaled(x/theta) value of tumor number density at initial time
        F(1,1)=beta*x(1,1)-mu;
```

```
        F1(1,1)=beta*x(1,1).*(0.4423-x(1,1));
for n=1
 for i=2:J+1
    r(i)=r(i-1)+dr;
    x(i,1)=0.9;
    F(i,1)=beta*x(i,1)-mu;
    F1(i,1)=beta*x(i,1).*(0.4423-x(i,1));
    u(1,1)=0;%Boundary condition of u.
    u(i,1)=((((r(i-1)*(R(1)-R_a))+R_a).^2)/(((r(i)*(R(1)-R_a))+R_a).^2))...
        *(u(i-1,1)+F(i-1,1)*dr);
            %Forward Euler's equation
 end
 for i=2:J
    A(1,1)=0;%At r=0
    A(i,1)=(1/(R(1)-R_a))*(u(i,1)-(r(i)*u(J+1,1)));%Forward Euler's equation
    A(J+1,1)=0; %Boundary condition for A at r=1
end
end
for n=2:49999;
    t(n)=t(n-1)+dt;
   %Defining radiotherapy and chemotherapy killing rate step functions
       if t(n)>=6 && t(n)<=12
          rho(n)=1;
       else rho(n)=0;
       if t(n)>=6 && t(n)<=12
         tau(n)=1;
      else if t(n)>=16 && t(n)<=20
            tau(n)=2;
      else if t(n)>=20 && t(n)<=40
            tau(n)=8/3;
      else tau(n)=0;
          end
          end
```

```
      end


       end
        for i=2:J
            r(i)=r(i-1)+dr;
           R(n)=R(n-1)+dt*((R(n-1)-R_a)*u(J+1,n-1));%Euler'sforward equation
           x(1,n)=(dt*F1(1,n-1))+x(1,n-1);%Boundary condition of x.
%            x(i,n)=x(i,n-1)+(dt)*(F1(i,n-1)-((A(i,n-1)*(x(i+1,n-1)...
% -x(i-1,n-1)))/(2*dr)));
              %Forward difference in time and central difference in r(FTCS)
           x(i,n)=(1/2)*(x(i+1,n-1)+x(i-1,n-1))+(dt)*(F1(i,n-1)...
               -((A(i,n-1)*(x(i+1,n-1)-x(i-1,n-1)))/(2*dr)));
               % FTCS is uncondionally unstable but it can be improved by
               % replacing x(i,n-1) by its spatial average (Lax method)
           x(J+1,n)=x(J+1,n-1)+dt*F1(J+1,n-1); %Boundary condition of x.
           F(1,n)=beta*x(1,n)-mu;
           F(i,n)=beta*x(i,n)-mu;
           F(J+1,n)=beta*x(J+1,n)-mu;
%   %Without Radiotherapy and Chemotherapy
%           F1(1,n)=beta*x(1,n)*((0.4423)-x(1,n));
%           F1(i,n)=beta*x(i,n)*((0.4423)-x(i,n));
%           F1(J+1,n)=beta*x(J+1,n).*((0.4423)-x(J+1,n));
  %With radiotherapy only (using A1)
         F1(1,n)=beta*x(1,n)*(0.4423-(A1*rho(n)/beta)-x(1,n));
        F1(i,n)=beta*x(i,n)*(0.4423-(A1*rho(n)/beta)-x(i,n));
        F1(J+1,n)=beta*x(J+1,n)*(0.4423-(A1*rho(n)/beta)-x(J+1,n));
%
         %With radiotherapy only  (using LQ model value)
              % Killing rate is multiplied by 7 to express rate in per
              % weeks.
%           F1(1,n)=beta*x(1,n)*(0.4423-(7*rho(n)/beta)*...
%           (1-exp(-alpha*(d+((d^2)/(n_frac*10)))))-x(1,n));
%         F1(i,n)=beta*x(i,n)*(0.4423-(7*rho(n)/beta)*...
```

```
%                 (1-exp(-alpha*(d+((d^2)/(n_frac*10)))))-x(i,n));
%         F1(J+1,n)=beta*x(J+1,n)*(0.4423-(7*rho(n)/beta)*...
%                 (1-exp(-alpha*(d+((d^2)/(n_frac*10)))))-x(J+1,n));

     %With radiotherapy and chemotherapy
%          F1(1,n)=beta*x(1,n)*(0.4423-(1/beta)*(7*rho(n)*...
%              (1-exp(-alpha*(d+((d^2)/(n_frac*10)))))+B*tau(n))-x(1,n));
%          F1(i,n)=beta*x(i,n)*(0.4423-(1/beta)*(7*rho(n)*...
%              (1-exp(-alpha*(d+((d^2)/(n_frac*10)))))+B*tau(n))-x(i,n));
%          F1(J+1,n)=beta*x(J+1,n)*(0.4423-(1/beta)*(7*rho(n)*...
%              (1-exp(-alpha*(d+((d^2)/(n_frac*10)))))+B*tau(n))-x(J+1,n));
%      F1(1,n)=beta*x(1,n)*((0.4423-(0.1756)*(A1*rho(n)+B*tau(n)))-x(1,n));
%     F1(i,n)=beta*x(i,n)*((0.4423-(0.1756)*(A1*rho(n)+B*tau(n)))-x(i,n));
% F1(J+1,n)=beta*x(J+1,n).*((0.4423-(0.1756)*(A1*rho(n)+B*tau(n)))-x(J+1,n));

            u(1,n)=0;
            u(i,n)=(((r(i-1).*(R(n)-R_a))+R_a).^2)/(((r(i).*(R(n)-R_a))...
                +R_a).^2)*(u(i-1,n)+F(i-1,n)*dr);
            u(J+1,n)=u(J,n)+F(J,n)*dr;
        end
        for i=2:J
            A(1,n)=0;
            A(i,n)=(1/(R(n)-R_a))*(u(i,n)-(r(i)*u(J+1,n)));
            A(J+1,n)=0;
        end
end

%  h=surf(t,lambda,x);
%   set(h,'LineStyle','none')
%  xlabel('time(weeks)')
%   ylabel('radial distance')
% ylabel('Alpha-beta ratio(H)')
%  ylabel('proliferation rate(y)')
```

```
%  zlabel('tumor cell density(cells/mm3)')
% title('tumor cell density surface plot with time and radial distance')
% title('tumor cell density surface plot with time and alpha-beta ratio')
% title('tumor cell density surface plot with time and radial distance')
% plot(t,tau)
plot(t,R,'b','linewidth',1.5)
%    plot(t, R);
   axis([0, 100, 15, 50])
ylabel('Tumor radius(mm)','fontweight','bold')
xlabel('Time(Weeks)','fontweight','bold')
title('Partial resection R*=18 mm; regrowth with radiotherapy')
 legend('alpha=0.137/Gy, A=1.687/week')
```

# APPENDIX B

## MATLAB SCRIPT: REACTION-DIFFUSION MODEL

```
% Numerical solution:
% Equations related
% Reaction-diffusion model in spherical coordinates with spherical symmetry.
% Neumann boundary conditions are used.To overcome divergence at r=0 in 2nd
% term of RHS, L'Hospital rule is used.
% dc/dt=D((d^2 c)/(dr^2 )+2(dc/dr)/r+(y-R)c(1-c/K)
clear
clc
%constant parameters
   y=0.035;         %Tumor cells Proliferation rate (in per day)
    K=1.96*(10^6);   %Carrying capacity in per mm^3(assumed constant in
                     %this model
    D=0.022;          %Diffusion coefficient in mm^2/day
    r0=25;           % A constant.This is center of gaussian distribution
    A=1/7;           %Radiotherapy killing rate, R(in per day)
    B=0.0260;        %B=D*dt/(dr^2)
    C=0.0013;        %C=D*dt/dr
    e=0.01;          %standard deviation of initial gaussian profile of
                     %tumor number density
     alpha=0.03;     %Radiosensitivity parameter
     d=2;            %Dose per fraction
    n_frac=30;       %Number of fractions for the delivery of radiation
                     %dose equal to 60Gy in total with 2Gy daily
%Discretizing net proliferation rate and alpha/beta ratio.
%   dy=0.001;         %proliferation rate step
%   M=10;             %number of iteration for  proliferation rate
  dH=0.01;          %alpha/beta ratio(H) step
%    Q=1000;             %number of iteration for H.
```

```
%Discretizing radial distance and time.
    ri=0;            %Initial value of radial distance
%   rf=100;
    dr = 0.1;        % Radial distance step
%     J=1000;%(rf-ri)/dr;    %Number of iteration of radial distance
    dt = 0.05;       %time step. CFL criteria demands D*dt<dr^2/2
     M=500;         % Number of iteration of time.

%Initializing matrix
    r = zeros(M+1,1);
    t = zeros(M+1,1);
    c = zeros(M+1,M+1);
    rho = zeros(M+1,1);
%     X=zeros(M+1,1);
    V=zeros(M+1,1);
%       y=zeros(M+1,1); %Discretization of tumor proliferation rate
     H=zeros(M+1,1);%Discretization of alpha/beta
% S=zeros(J+1,1);
%Initializing alpha-beta ratio
%   y(1)=0.001;         %Initial tumor cells Proliferation rate (in per days)
     H(1)=8;          %Initial value of alpha beta ratio
%          for j=2:M+1   %loop for variable net proliferation rate (y)
%          y(j)=y(j-1)+dy;

       for l=2:M+1      %loop for alpha/beta ratio(H)
      H(l)=H(l-1)+dH;
     %Initializing values
    t(1) = 0;        % the initial condition for time
    r(1)=0;          % the initial condition for radial distance
    c(1,1)=(1/(sqrt(2*pi)*e))*exp((-1/2)*((r0/e)^2));
                     % Initial concentration at r=0 and t=0,

for i=2:M+1
```

```
    r(i)=r(i-1)+dr;
    c(i,1)=(1/(sqrt(2*pi)*e))*exp((-1/2)*(((r(i)-r0)/e)^2));
                      %Gaussian profile for inital cell density.
end
for n=2:M+1;
    t(n)=t(n-1)+dt;
         if t(n)>=42 && t(n)<=84
                     %Defining radiotherapy killing rate step function.
               rho(n)=1;
         else rho(n)=0;
         end

%  for i=2:M
% %Formula for tumor cell density
% c(i,n)=(1-2*B)*c(i,n-1)+(B+(C/r(i)))*c(i+1,n-1)+(B-(C/r(i)))*c(i-1,n-1)...
%  +dt*(y(j)-(1-exp(-alpha*(d+((d^2)/(n_frac*10)))))*rho(n))...
%  *c(i,n-1)*(1-(c(i,n-1))/K);
% end
% %Boundary condition at r(1)
%    c(1,n) = c(1,n-1)+6*B*(c(2,n-1)-c(1,n-1))+dt*(y(j)-(1-exp(-alpha*...
%  (d+((d^2)/(n_frac*10)))))*rho(n))*c(1,n-1)*(1-(c(1,n-1))/K);
% %Boundary condition at r(J+1)
%    c(M+1,n)=(1-2*B)*c(M+1,n-1)+2*B*c(M,n-1)+dt*(y(j)-(1-exp(-alpha*...
%  (d+((d^2)/(n_frac*10)))))*rho(n))*c(M+1,n)*(1-(c(M+1,n-1))/K);
% end

 for i=2:M
%  %Without therapy
%         c(i,n)=(1-2*B)*c(i,n-1)+(B+(C/r(i)))*c(i+1,n-1)+(B-(C/r(i)))...
%            *c(i-1,n-1)+dt*c(i,n-1)*(1-(c(i,n-1))/K));%Without therapy
% end
% %Boundary condition at r(1)
%      c(1,n)=c(1,n-1)+6*B*(c(2,n-1)-c(1,n-1))+dt*c(1,n-1)*(1-(c(1,n-1))/K);
```

```
% % Boundary condition at r(J+1)
%  c(J+1,n)=(1-2*B)*c(J+1,n-1)+2*B*c(J,n-1)+dt*c(J+1,n)*(1-(c(J+1,n-1))/K);

% For variable alpha/beta(H)ratio
% %Formula for tumor cell density
 c(i,n)=(1-2*B)*c(i,n-1)+(B+(C/r(i)))*c(i+1,n-1)+(B-(C/r(i)))*c(i-1,n-1)...
 +dt*(y-(1-exp(-alpha*(d+((d^2)/(n_frac*H(l-1))))))*rho(n))...
 *c(i,n-1)*(1-(c(i,n-1))/K);
end
% %Boundary condition at r(1)
    c(1,n) = c(1,n-1)+6*B*(c(2,n-1)-c(1,n-1))+dt*(y-(1-exp(-alpha*...
  (d+((d^2)/(n_frac*H(l-1))))))*rho(n))*c(1,n-1)*(1-(c(1,n-1))/K);
% %Boundary condition at r(J+1)
      c(M+1,n)=(1-2*B)*c(M+1,n-1)+2*B*c(M,n-1)+dt*(y-(1-exp(-alpha*...
  (d+((d^2)/(n_frac*H(l-1))))))*rho(n))*c(M+1,n)*(1-(c(M+1,n-1))/K);
 end
 X=c(:,30);
  V=[V X];
  end
%  h=surf(t,r,c);
 h=surf(r,H,V);
 set(h,'LineStyle','none')
% xlabel('time(days)')
 xlabel('radial distance (mm)')
 ylabel('Alpha-beta ratio(Gy)')
%  ylabel('Net proliferation rate(y)')
zlabel('tumor cell density(cells/mm3)')
% title('tumor cell density surface plot with time and radial distance')
 title('tumor cell density surface plot with radial distance and alpha-beta ratio')
% title('tumor cell density surface plot with time and net proliferationrate')
 axis ([0 50 9 11 0 50])
```

# APPENDIX C

## MATLAB SCRIPT: ANTI-ANGIOGENIC THERAPY MODEL

```
% Equations related
% dV(t)/dt=-lambda*V(t)*log(V(t)/K(t))
%dK(t)/dt=b*V(t)-d*K(t)*(V(t)^2/3)
%Define constant parameters
clear
clc
lambda=0.192;% tumor growth coefficient(day^-1)
g1=20;
  b=5.85;%Angiogenesis stimulatory rate (day^-1)
%  d=0.00873;% Rate of angiogenesis inhibition(day^-1)
e=1.3;%Rate of concentration ofchemotherapy inhibition(conc^-1.day^-1)
%Stimulatory rate(b), Inhibitory rate(d),time step and number of iterations
% db=0.005;
 dd=0.000005;
 N=1000;
 dt=0.05;
%Initialize matrix
t=zeros(N,1);
V=zeros(N,1);
K=zeros(N,1);
%  b=zeros(N,1);
 d=zeros(N,1);
Y =zeros(N+1,1);
%Initial parameters
%   b(1)=3;
 d(1)=0.004;
%Run loop
% for j=1:N
```

```
%      b(j+1)=b(j)+db;
     for k=1:N
     d(k+1)=d(k)+dd;
t(1)=0;
V(1)=200; %Initial volume of tumor (mm^3).
K(1)=625; %Initial carrying capacity (mm^3).
    for i=1:N
        t(i+1)=t(i)+dt;

        %Using Euler forward methodfor dV/dt
              V(i+1)=V(i)-lambda*dt*V(i)*log(V(i)/K(i));
        %Using Euler forward method for dK/dt
        %For variable d
              K(i+1)=K(i)+b*dt*V(i)-d(k)*dt*K(i)*(V(i).^(2/3));
        %For variable b
%              K(i+1)=K(i)+b(j)*dt*V(i)-d*dt*K(i)*(V(i).^(2/3));

    end
     Y=[Y V];
%     Y=[Y V];
    end

  h1=surf(t,d,Y);
   xlabel('time(days)','fontweight','bold')
      set(get(gca,'xlabel'),'Rotation',+15);
   ylabel('Inhibitory rate(per days)','fontweight','bold')
    set(get(gca,'ylabel'),'Rotation',-25);
   zlabel('Tumor volume (mm^3)','fontweight','bold')
      title('Surface plot of V with variable d and t')
```

## BIBLIOGRAPHY


[1] Glioma — American Brain Tumor Association

[2] H.L.P. Harpold, E.C. Alvord, K.R. Swanson *The Evolution of Mathematical Modeling of Glioma Proliferation and Invasion* J Neuropathol Exp Neurol **66** (2007) pp. 1-9.

[3] http://www.neurooncology.ucla.edu/

[4] http://oerpub.github.io/epubjs-demo-book/content/m46509.xhtml

[5] The cell cycle in cancer- developing cancer therapies to stop the growth of cancer cells — Cyclacel

[6] H.Hatzikirou et al. *'Go or Grow': the key to the emergence of invasion in tumor progression?* Mathematical Medicine and Biology (2010) 1-17.

[7] https://oncogenesandcancer.wordpress.com/cell-cycle-checkpoints-and-effect-of-oncogenes-2/

[8] B. Fredereque, J. Clairambault, O. Fercoq *Optimisation of Cancer Drug Treatments Using Cell Population Dynamics* pp.5-6.

[9] P. Hahnfeldt. D. Panigrahy, J. Folkman, L. Hlatky *Tumor Development under Angiogenic Signaling: A Dynamical Theory of Tumor Growth, Treatment Response, and Postvascular Dormancy* Cancer Research 59 (1999).

[10] K.R. Swanson et al. *Quantifying the role of angiogenesis in malignant progression of gliomas: In silico modeling integrates imaging and histology.* Cancer Res. 71(24) (2011).

[11] R.C. Rockne *Towards Patient-Specific Mathematical Radiation Oncology* .University of Washington (2013).

[12] J.D. Murray. *Mathematical Biology II: Spatial Models and Biomedical Applications.*Springer. Third Edition (2003) .

[13] J.P. Tian, A. Friedman, J. Wang, E.A. Chiocca. *Modeling the effects of resection, radiation and chemotherapy in glioblastoma* J Neurooncol **91** (2009) 287-293.

[14] D. Corwin, C. Holdsworth, R.C. Rockne, A.D. Trister, M.M. Mrugala, J.K. Rockhill, R.D. Stewart, M. Philips, K.R. Swanson. *Toward Patient-Specific, Biologically Optimized Radiation Therapy Plans for the Treatment of Glioblastoma.* PLOS ONE **8** (2013).

[15] M. Le, H. Delingette, J.K- Cramer, E. Gerstner, H.A. Shih ..et al. *Multimodal Analysis of Vasogenic Edema in Glioblastoma Patients for Radiotherapy Planning.*Workshop Image-Guided Adaptive Radiation Therapy (2014) .

[16] Zhang, Jenny Z. and Bryce, Nicole S. and Siegele, Rainer and Carter, Elizabeth A. and Paterson, David and de Jonge, Martin D. and Howard, Daryl L. and Ryan, Chris G. and Hambley, Trevor W. *The use of spectroscopic imaging and mapping techniques in the characterisation and study of DLD-1 cell spheroid tumour models* Integr. Biol **4** (2012) 1072-1080.

[17] J. Unkelbach, B.H. Menze, E. Konukoglu, F. Dittmann, N. Ayache,H.A. Shih *Radiotherapy planning for glioblastoma based on a tumor growth model: implications for spatial dose redistribution* Physics in Medicine and Biology **69** (2014) .

[18] J. Unkelbach, B.H. Menze, E. Konukoglu, F. Dittmann, N. Ayache,H.A. Shih, M. Le. *Radiotherapy planning for glioblastoma based on a tumor growth model: Improving target volume delineation* arXiv:1311.5902 [physics.med-ph] ***v*2** (2013).

[19] E. Konukoglu. *Modeling Glioma Growth and Personalizing Growth Models in Medical Imagesl* Thesis, University of Nice - Sophia Antipolis (2009).

[20] E. Mandonnet, J. Pallud, O. Clatz, L. Tailandier, E. Konukoglu, H. Duffau, L. Capelle. *Computational modeling of the WHO grade II glioma dynamics: principles and applications to management paradigm.*Neurosurg Rev **31** (2008) 263-269.

[21] E. Ozugurlu. *A note on the numerical approach for the reaction-diffusion problem to model the density of the tumor growth dynamics.*Computer and Mathematics with Applications **69** (2015) 1504-1517.

[22] J.P. Tian, K. Stone, T.J. Wallin. *A Simplified Mathematical Model of Solid Tumor Regrowth with Therapies* DISCRETE AND CONTINUOUS DYNAMICAL SYSTEMS Suppliment (2019) 771-779.

[23] D. Yang, J.P. Tian, J. Wang. *A solvable hyperbolic free boundary problem modelling tumour regrowthl* Applicable Analysis: An International Journal **10** (2012).

[24] J. Folkman, R. Kalluri. http://web.mit.edu/hst527/www/readings/Lecture

[25] Y. Cao, R. Langer. *A review of Judah Folkman's remarkable achievements in biomedicine* PNAS **105** (2008).

[26] M. Lacroix, D. Abi-Said, D.R. Fourney, Z.L. Gokaslan, W. Shi, F. DeMonte et al. *A multivariate analysis of 416 patients with glioblastoma multiforme: prognosis, extent of resection, and survival* J Neurosurg.**95** (2001) 190-198.

[27] A. Porter. *A Dead End: A Review of Glioblastoma Multiforme* Eukaryon, Lake Forest College.**8** (2012).

[28] http://www.irsa.org/glioblastoma.html

[29] F.K. Albert, M. Forsting, K. Sartor, H.P. Adams, S. Kunze. *Early postoperative magnetic resonance imaging after resection of malignant glioma: objective evaluation of residual tumor and its influnce on regrowth and prognosis*Neurosurgery **34** (1994) 45-61.

[30] R. Rockne et al. *Predicting efficacy of radiotherapy in individual glioblastoma patients in vivo: a mathematical modelling approach*Phys Med Biol. **55** (2010).